

2018 • 2019  
Faculteit Industriële ingenieurswetenschappen  
master in de industriële wetenschappen: biochemie

## Masterthesis

Biotechnological Production of Nanobodies Against Epithelial  
Ovarian Cancer

PROMOTOR :

dr. Geert-Jan GRAULUS

PROMOTOR :

Prof. dr. Wanda GUEDENS

BEGELEIDER :

ing. Orpha BAILLIEN

BEGELEIDER :

Mevr. Huong TRAN

Anneleen Coun

Scriptie ingediend tot het behalen van de graad van master in de industriële wetenschappen: biochemie

Gezamenlijke opleiding UHasselt en KU Leuven



2018 • 2019

Faculteit Industriële ingenieurswetenschappen  
master in de industriële wetenschappen: biochemie

## Masterthesis

Biotechnological Production of Nanobodies Against Epithelial  
Ovarian Cancer

**PROMOTOR :**

dr. Geert-Jan GRAULUS

**PROMOTOR :**

Prof. dr. Wanda GUEDENS

**BEGELEIDER :**

ing. Orpha BAILLIEN

**BEGELEIDER :**

Mevr. Huong TRAN

### Anneleen Coun

Scriptie ingediend tot het behalen van de graad van master in de industriële wetenschappen: biochemie



**KU LEUVEN**



## Preface

In the last year of my education in biomedical laboratory technology, I realized that I became more interested in the theory of everything instead of the practical work. During my internship at the hospital as clinical laboratory technician, I was wondering how every device was working and how it could become more efficient. At that point, I decided to start a 'preparatory programme' for the master of biochemical engineering technology. It was a difficult and hard adjustment between both educations, but I am glad that I made the decision. This thesis is the last step towards my graduation. It is based on my research during my internship in the Biomolecule Design Group at UHasselt. During this period, I tried to find optimal settings for the biotechnological production of nanobodies that can be used in diagnostic tools. In this work, you can find the background of the project, the used techniques and the results.

First, I would like to thank my external promotor dr. Geert-Jan Graulus for his support and guidance during my internship and thesis. I learned a lot of his experience and knowledge and I am sure this has contributed to my development as engineer. Because of him, I also improved my English writing skills. Apart from the fact that he is a motivative promotor, he is also an excellent lecturer. During his lectures, I learned a lot more about recombinant DNA to use this during my research. In addition, I also want to thank Huong Tran for teaching me the practical work, including the small tips and tricks.

I would like to express my gratitude towards my internal promotor Prof. dr. Wanda Guedens. Even before my internship, she took the time to give me a full explanation about the subject of my thesis. During my internship and writing process, she was always willing to help. I would also like to thank ing. Orpha Baillien for the follow-up and interest she had in my thesis. Her corrections helped to complete this thesis.

Furthermore, I can't thank my parents enough for giving me the opportunity and courage to study. They financially supported me during my education, but their emotional support was equally important and strengthened me over and over again. In hard times, they were always there to listen and encourage me not to give up. They are my role models and because of them, I made it through university. Besides my parents, I am also thankful for my whole family and friends to motivate me. Thanks a million especially to my fellow students Julie Boonen, Demi Renders, Isabelle Van Dyck and Wouter Van Genechten for the helping hand and advice.

Finally, I would like to thank my girlfriend Sofie Vanlommel to walk this road with me. Her motivational words and encouragement were a great support in difficult times.



# Table of contents

Preface .....	1
List of tables.....	5
List of figures.....	7
Abbreviations.....	9
Abstract .....	11
Abstract in Dutch .....	13
1 Introduction .....	15
2 Epithelial ovarian cancer.....	19
2.1 Treatment.....	21
2.2 Diagnosis .....	21
2.3 Biomarkers.....	21
3 Biosensing .....	23
3.1 Nanobodies .....	25
3.2 Protein expression.....	26
3.3 Intein-mediated protein ligation .....	28
4 Material and methods.....	31
4.1 Preparation of the agar plates and media .....	31
4.2 Parameter-dependent protein expression .....	32
4.3 SDS-PAGE.....	33
4.4 Purification .....	33
4.5 Nanodrop .....	35
5 Results and discussion.....	37
5.1 Parameter-dependent fusion protein expression .....	37
5.2 Purification .....	40
5.3 Nanodrop .....	41
6 Conclusion .....	43
References .....	45
Appendices.....	49



## List of tables

Table 1: Clinically relevant EOC biomarker concentrations .....	15
Table 2: Subdivisions tumor staging .....	20
Table 3: The obtained chemicals and reagents, other from Sigma-Aldrich.....	31
Table 4: The varied expression parameters .....	32
Table 5: The varied purification parameters.....	35
Table 6: The optimal parameter settings for protein expression .....	43





## List of figures

Figure 1: Schematic representation of a biosensor.....	23
Figure 2: A) The setup of a SPR sensor in the Kretschmann configuration. B) Typical SPR curve with the reflected intensity in function of the incident angle. The curves represent the spectrum of the reflected light before and after refractive index change .....	24
Figure 3: Schematic representation of an IgG antibody .....	25
Figure 4: Difference between a conventional Ab (left), an HCAb (middle) and a Nb (right).....	26
Figure 5: The schematic representation of genetic recombination .....	27
Figure 6: The schematic presentation of the lac operon.....	28
Figure 7: The schematic representation of the fusion protein construct .....	28
Figure 8: The IPL mechanism.....	30
Figure 9: The copper(I)-catalyzed azide/alkyne cycloaddition (CuAAC).....	30
Figure 10: The principle of the SDS-PAGE result of the Nb purification after fusion protein expression in <i>E. coli</i> .....	34
Figure 11: Temperature-dependent fusion protein expression .....	37
Figure 12: IPTG concentration-dependent fusion protein expression .....	38
Figure 13: Time-dependent fusion protein expression .....	39
Figure 14: Medium-dependent fusion protein expression .....	39
Figure 15: Fusion protein expression with the optimal parameter settings .....	40
Figure 16: Purification SDS-PAGE results of strain 2210 .....	50
Figure 17: Results of the Nb concentration measurements through Nanodrop of strain 2210.....	50
Figure 18: Purification SDS-PAGE results of strain 2276 .....	50
Figure 19: Results of the Nb concentration measurements through Nanodrop of strain 2276.....	51
Figure 20: Purification SDS-PAGE results of strain 3237 .....	51
Figure 21: Results of the Nb concentration measurements through Nanodrop of strain 3237.....	51
Figure 22: Purification SDS-PAGE results of strain 2276 .....	52
Figure 23: Results of the Nb concentration measurements through Nanodrop of strain 2276.....	52
Figure 24: Purification SDS-PAGE results of strain 2210 .....	53
Figure 25: Results of the Nb concentration measurements through Nanodrop of strain 2210.....	53
Figure 26: Purification SDS-PAGE results of strain 3237 .....	53
Figure 27: Results of the Nb concentration measurements through Nanodrop of strain 3237.....	54
Figure 28: Purification SDS-PAGE results of strain 2276 .....	54
Figure 29: Results of the Nb concentration measurements through Nanodrop of strain 2276.....	54



## Abbreviations

EOC	Epithelial ovarian cancer
Abs	Antibodies
Ags	Antigens
APS	Ammonium persulfate
B-PER	Bacterial protein extraction reagent
CA-125	Cancer antigen 125
CB	Column buffer
CBD	Chitin-binding domain
CDR	Complementary determining region
CH	Constant domain of the heavy chain
CL	Constant domain of the light chain
CuAAC	Copper-catalyzed azide-alkyne cycloaddition
DMF	N, N-dimethylformamide
DTT	Dithiothreitol
<i>E. coli</i>	<i>Escherichia coli</i>
EDC	1-Ethyl-3-(3-dimethylaminopropyl)
EDTA	Ethylenediaminetetraacetic acid
Fab	Antigen-binding fragment
GLB	Gel loading buffer
HCAbs	Heavy chain antibodies
H-chain	Heavy-chain
HE4	Human epididymis secretory protein 4
HEPES	4-(2-hydroxyethyl) -1-piperazineethanesulfonic acid
IgG	Immunoglobulin gamma
Igs	Immunoglobulins
IPL	Intein-mediated protein ligation
IPTG	Isopropyl $\beta$ -D-1-thiogalactopyranoside
LB	Luria-Bertani
L-chain	Light-chain
MESNA	2-mercaptoethanesulfonic acid
Milli-Q water	Distilled water
Nb/Nbs	Nanobody/Nanobodies
NHS	N-hydroxysuccinimide
PBS	Phosphate-buffered saline
PGRN	Progranulin
SDS	Sodium dodecyl sulphate
SDS-PAGE	Sodium dodecyl sulphate polyacrylamide gel electrophoresis
SLPI	Secretory leukocyte protease inhibitor
SPE	Solid phase extraction
SPR	Surface plasmon resonance
TB	Terrific Broth
TEMED	Tetramethylethylenediamine
THF	Tetrahydrofuran
TYP	Tryptone yeast peptone
VH	Variable domain of the heavy chain

VHH	Variable domain of the heavy chain of the heavy chain antibodies
VL	Variable domain of the light chain

## Abstract

Epithelial ovarian cancer (EOC) is the fourth most common cause of female cancer death in the world. It is desirable to detect EOC in an early stage to increase survival rate and reduce side effects of chemotherapy. Studies have shown that HE4, PGRN and SLPI are potential biomarkers for EOC. Nanobodies, derived from camelid antibodies, are an ideal tool for the detection of these biomarkers in biosensing tools due to their small size, high stability and easy genetic manipulation.

The aim of this study is to optimize the biotechnological production of nanobodies, wherein *Escherichia coli* is used for expression. The expression step can be combined with the intein-mediated protein ligation technique to yield a nanobody modified with an alkyne function. This function can be used for the immobilization of the nanobodies on biosensor surfaces. In a first part, the expression parameters (temperature, time, medium and concentration of expression inducer) were optimized. In a second part, the downstream purification of the expressed protein via affinity chromatography based on a chitin column was studied.

SDS-PAGE results of the first part show that the highest protein expression is achieved at 37°C, in LB or TB medium, for 2-3 hours and with a concentration of 0.1 mM inducer. The purification results show that further research is needed.

First developments towards the production of pure nanobodies targeting the above-mentioned biomarkers were conducted.



## Abstract in Dutch

Epitheliale eierstokkanker is de vierde meest voorkomende doodsoorzaak bij vrouwen met kanker ter wereld. Om de bijwerkingen van chemotherapie te verminderen en de overlevingskansen te verhogen, dient de kanker in een vroeg stadium opgespoord te worden. HE4, PGRN en SLPI zijn veelbelovende biomerkers voor de detectie van epitheliale eierstokkanker. Nanobodies, afkomstig van kameelachtigen, zijn een ideale tool om de eerder genoemde biomerkers op te sporen met behulp van biosensoren. Dit dankzij hun kleine afmetingen, hoge stabiliteit en makkelijke genetische manipulatie.

Het doel van deze thesis is om de biotechnologische productie van nanobodies in *Escherichia coli* te optimaliseren. De expressie kan worden gecombineerd met intein-mediated protein ligation om een alkyn-gemodificeerde nanobody te krijgen dat gebruikt kan worden voor de immobilisatie in biosensoren. De expressie werd geoptimaliseerd aan de hand van verschillende expressieparameters (temperatuur, tijd, medium, concentratie expressie-inducer). De opzuivering van nanobodies gebeurde vervolgens via affiniteitschromatografie op basis van een chitine kolom.

De SDS-PAGE resultaten van de expressie geven weer dat de hoogste expressie wordt waargenomen bij 37°C, in LB of TB medium, gedurende 2 tot 3 uren en met een concentratie van 0,1 mM inducer. De resultaten van de opzuivering tonen aan dat verder onderzoek noodzakelijk is.

Dankzij de bekomen resultaten staat men een stap dichterbij de beoogde nanobody sensoren.





# 1 Introduction

The Biomolecule Design Group (BDG) is a research group that is part of the Institute of Materials Research (IMO) at University of Hasselt. BDG investigates among others the site-specific bio-orthogonal modification of nanobody proteins or Nanobodies® (Nbs). Nbs are derived from camelids antibodies and are widely used in diagnostic and therapeutic applications [1] [2].

A lot of research has been done using Nbs in the detection of cancer biomarkers, but Nbs concerning epithelial ovarian cancer (EOC) have not been studied in great detail. The Globocan study reported that in 2012 worldwide there were approximately 239,000 women diagnosed with EOC and about 152,000 patients died from this disease [3]. These estimations represent 3.6% of cancer cases and 4.3% of cancer deaths, respectively. The Globocan study also estimates that by the year 2035, the number of cases and deaths will increase to 371,000 and 254,000, respectively. These predictions are made by using UN World Population Prospects and applying Age Standardized Rates. There are a lot of elements that affect the risk and mortality rates of EOC e.g. ethnicity, tumor type and patient age [3].

EOC generally presents itself in postmenopausal women with symptoms as abdominal pain and distension. When the cancer remains untreated due to the late presentation of symptoms and therefore the late diagnosis, patients will die from malignant bowel obstruction in ways that are not amenable to surgery. When the cancer is detected, mostly in an advanced stage, chemotherapy constitutes the standard course of treatment. Nevertheless, chemotherapy is associated with heavy side effects and is therefore not desirable [4]. To improve the survival rate and allow for treatment based on milder chemotherapeutics, it is important to detect and diagnose EOC in an early stage. However, robust detection methods are still missing. The sensitivity and specificity of the detection methods has to be high enough (higher than 75% and 99.6%, respectively) to provide accurate results [5].

Biomarkers are biomolecules that can be used to diagnose metabolic diseases like cancer, since cancer induces changes in the concentration of certain metabolites [6]. Human epididymis protein 4 (HE4), secretory leukocyte protease inhibitor (SLPI) and progranulin (PGRN) are specific biomarkers for EOC [7]. These biomarkers are proteins which are present in deviating concentrations in EOC patients' serum. Table 1 shows the difference in biomarker concentrations between healthy women and EOC patients [8]–[10].

Table 1: Clinically relevant EOC biomarker concentrations, adapted from [8]–[10]

	<b>HE4</b>	<b>SLPI</b>	<b>PGRN</b>
<b>EOC patients</b>	>150 pM	67 ng/ml	> 59 ng/ml
<b>Healthy women</b>	<150 pM	32 ng/ml	< 59 ng/ml

In this project, Nbs are a tool to target the mentioned EOC specific biomarkers through biosensors. Ta *et al.* reported that "Nbs have a great potential due to numerous advantages over the conventional antibodies: small size, high stability and easy genetic manipulation and expression in *Escherichia coli* (*E. coli*) " [11, p. 2]. At this point, the aim of biosensing is to detect and quantify the specific biomarkers in a patient's serum at clinically relevant concentrations based on modified Nbs.

Modified Nbs can be easily expressed in *E. coli* through cytoplasmic or periplasmic expression. Periplasmic expression usually results in expressed proteins, which are less susceptible to proteolysis and need milder down-stream purification protocols than cytoplasmic expression. In order for the protein to be transported to the periplasm, an N-terminal signal peptide is required. However, periplasm expression has several drawbacks, including an inefficient translocation of proteins, partially processed proteins and abbreviated leader sequences. Therefore, cytoplasmic expression experiments usually result in higher yields. After the expression, it is essential that the protein of interest can be purified, e.g. based on chitin columns, from other components and proteins. [12].

The performance of biosensors relies on the site-specific, covalent immobilization of the Nbs on a specific surface in a controllable way to ensure the orientation is optimal for biomarker binding. Therefore, the Nbs have to be provided with an extra chemical function, for example an alkyne function, to be used in diagnostic tools, e.g. detection of EOC biomarkers with biosensing. The introduced alkyne moiety is available to react with a molecule that contains an azide group, present on a biosensor surface [13]. At this point, the coupling between the modified Nb and the biosensor surface is implemented. As mentioned above, it is desirable that EOC can be detected in an early stage through biomarkers that can bind the Nbs at the antigen-binding site [13]. The interaction between Nb and biomarker can be detected by a wide array of techniques among others surface plasmon resonance (SPR) in which gold-coated sensor chips are essential [11].

Since previous studies have not dealt with the optimal parameters for cytoplasmic expression and purification based on chitin columns, the experiment parameters to reach a high yield of Nbs remain unclear. The aim of this research is to optimize the biotechnological production of Nbs against EOC. The yield has to be increased to a value higher than 5 mg/l, preferably approximately 20 mg/l, to be interesting in actual biosensor applications for the detection of EOC. This can be done by several strategies, but in this work two strategies will be examined:

1. The optimization of the protein expression procedure:

The standard protocol settings of the protein expression in *E. coli* will be optimized for the studied Nb strains. The expression parameters that will be varied are temperature, time, growth medium and the concentration of the inducing agent.

## 2. The optimization of the purification procedure:

The standard protocol settings of the purification through a chitin column will be optimized. Purification is done after expression to ensure that the engineered Nbs will be separated from the other proteins present in the solution. The parameters that will be varied are cleavage time and temperature.

Both strategies will be performed separately to determine the optimal settings for each strategy and the results will be evaluated with SDS-PAGE (sodium dodecyl sulphate polyacrylamide gel electrophoresis). In the end, the concentration of the purified Nbs will be measured.



## 2 Epithelial ovarian cancer

Epithelial ovarian cancer is a metabolic disease, which affects postmenopausal women. It is the sixth most common cancer in women and the fourth most common cause of female cancer death in the world [4], [5]. Nowadays, cancer is the main cause of human mortality next to heart failure. In 2015, Siegel *et al.* reported that death rates from different types of cancer may surpass congestive heart failure in the near future [14].

EOC is the result of the malignant conversion of the ovarian epithelium [5]. EOC is classified into two subtypes: Type I (low grade) and Type II (high grade). The difference between both is their progression of the tumor. It is known that low-grade tumors will grow more slowly in contrast to the high-grade tumors. High grade serous ovarian carcinoma (HGSCO) is an example of high-grade tumors and is one of the most aggressive ovarian cancers that represents 75% of all EOCs. Most of the time, EOC has evolved into a metastatic stadium, usually with metastases in the peritoneal cavity. This may be due to the lack of effective methods for early detection of HGSOC and the non-specific symptoms including vaginal bleeding, pain in the abdomen and more frequently urinating [15], [16].

In 2014, Prat published a paper with the staging classification for ovarian cancers, as proposed by the International Federation of Gynecology and Obstetrics (FIGO) [17]. The stage of the disease can be determined via a surgical procedure i.e. exploratory laparotomy [17], [18]. Prat reported the four different stages of EOC and the different subdivisions and they are given in Table 2 [17, p. 2-4].

An important risk factor for EOC is genetic in nature, which may be related to an inherited mutation. The mutation occurs in one or two genes, known as BRCA1 and BRCA2 which are located on chromosomes 17q and 13q, respectively. The mentioned genes can be inherited from both parents, thus it is important to gather an entire family history [18]. Other important risk factors include the early start of menstruation, nulliparity and late menopause. The risk to be diagnosed with EOC is lowered by the use of oral contraception, pregnancy and lactation [5].

It is important that women affected by EOC are treated with a specific therapy to increase their life expectancy. The following part will briefly summarize the standard procedure for treatment. For an extensive description of EOC treatment, reference is made to an excellent review by Eisenhauer [19].

Table 2: Subdivisions tumor staging, adapted from [17, p. 2-4]

<u>Stage I</u>	<p><u>Tumor confined to ovaries or fallopian tube(s)</u></p> <p>IA Tumor limited to one ovary or fallopian tube</p> <p>IB Tumor limited to one or both ovaries or fallopian tubes</p> <p>IC Tumor limited to one or both ovaries or fallopian tubes, with any of the following:</p> <ol style="list-style-type: none"> <li>1. Surgical spill</li> <li>2. Capsule ruptured before surgery or tumor on ovarian or fallopian tube surface</li> <li>3. Malignant cells in the ascites or peritoneal washings</li> </ol>
<u>Stage II</u>	<p><u>Tumor involves 1 or both ovaries or fallopian tubes with pelvic extension or primary peritoneal cancer</u></p> <p>IIA Extension and/or implants on uterus and/or fallopian tubes and/or ovaries</p> <p>IIB Extension to other pelvic intraperitoneal tissues</p>
<u>Stage III</u>	<p><u>Tumor involves 1 or both ovaries or fallopian tubes, or primary peritoneal cancer with cytologically or histologically confirmed spread to the peritoneum outside the pelvis and/or metastasis to the retroperitoneal<sup>1</sup> lymph nodes</u></p> <p>IIIA1 Positive retroperitoneal lymph nodes only:</p> <ol style="list-style-type: none"> <li>1. Metastasis up to 10 mm in greatest dimension</li> <li>2. Metastasis more than 10 mm in greatest dimension</li> </ol> <p>IIIA2 Microscopic extrapelvic (above the pelvic brim) peritoneal involvement with or without positive retroperitoneal lymph nodes</p> <p>IIIB Macroscopic peritoneal metastasis beyond the pelvis up to 2 cm in greatest dimension, with or without metastasis to the retroperitoneal lymph nodes</p> <p>IIIC Macroscopic peritoneal metastasis beyond the pelvis more than 2 cm in greatest dimension, with or without metastasis to the retroperitoneal lymph nodes (includes extension of tumor to capsule of liver and spleen without parenchymal involvement of either organ)</p>
<u>Stage IV</u>	<p><u>Distant metastasis excluding peritoneal metastases</u></p> <p>IVA Pleural effusion with positive cytology</p> <p>IVB Parenchymal metastases and metastases to extra-abdominal organs (including inguinal lymph nodes and lymph nodes outside of the abdominal cavity)</p>

<sup>1</sup> Anatomical space in the abdominal cavity behind the peritoneum

## 2.1 Treatment

If EOC is suspected based on physical examination and imaging, a surgical procedure will be performed by a gynecological oncology surgeon. The surgery, an exploratory laparotomy, will be performed for histological diagnosis, staging and tumor debulking. This may include a total abdominal hysterectomy<sup>2</sup> and bilateral salpingo-oophorectomy<sup>3</sup>. During the procedure, several medical operations will be performed, including biopsies of pelvic and para-aortic lymph nodes and examining the peritoneal surfaces. If a patient with stage IA or IC desires to preserve fertility, a unilateral salpingo-oophorectomy can be considered [4], [5]. When complete surgical debulking is not feasible, neoadjuvant (preoperative) chemotherapy is provided. After three of the six cycles chemotherapy, another debulking procedure will be done [4].

Since the 1980s, primary debulking surgery followed by chemotherapy has become a standard procedure to treat EOC [18], [20]. Chemotherapy is associated with severe side effects among others nausea, vomiting, taste alteration, weight loss and constipation [21]. Therefore, it is desirable to detect EOC in an early stage to avoid the side effects of long-term chemotherapy and to increase the survival rate of EOC patients. A full discussion of EOC treatment lies beyond the scope of this thesis. Reference is made to a paper of Houben and colleagues who previously covered this topic [22].

## 2.2 Diagnosis

EOC presents with three to four months of abdominal pain or distension, which are the same symptoms as found by patients with irritable bowel syndrome. Such non-specific symptoms may result in wrong diagnoses [4]. To ensure the correct diagnosis of EOC, several options to detect EOC are available. The results have to be evaluated together to conclude whether or not the patient is affected by EOC [5]. Transvaginal ultrasonography (TVS) is a first screening test that is often performed when EOC is suspected due to the patients' medical history and physical examination. The operation of TVS is based on high-frequency sound waves imaging internal organs (e.g. uterus, ovaries and fallopian tubes) [23]. When TVS indicates an ovarian cyst, the patient may be affected by EOC. Another screening test is based on membrane glycoproteins, which serve as biomarkers or tumor markers. Biomarkers are biomolecules secreted by cancer cells and measurement of deviating serum levels is an indication of the presence of a specific cancer [24]. TVS and measurement of biomarkers are performed together and if EOC is suggested, surgery is usually performed to make a conclusive, histopathological diagnosis and determine which stage is currently developed [4], [5].

## 2.3 Biomarkers

As previously mentioned, biomarkers are biomolecules secreted by cancer cells and are present in deviating concentrations in the serum samples of patients.

---

<sup>2</sup> Surgery to remove the uterus and cervix

<sup>3</sup> Surgery to remove both ovaries and both fallopian tubes



Therefore, biomarkers can be used in the diagnosis of several diseases including cancer. Biomarker cancer antigen 125 (CA-125) is the most commonly used tumor marker for the detection of EOC [25].

CA-125 concentration is raised in more than 80% of EOC patients. However, this assay alone is not sufficient to make a clear EOC diagnosis due to its low specificity. CA-125 is a glycoprotein produced by the mesothelial cells and as such, the concentration of CA-125 in serum can be increased by several medical causes other than EOC (e.g. congestive heart failure, cirrhosis, lung and breast cancer) [4], [5], [24]. Urban *et al.* reported that CA-125 has a high sensitivity (80%) for EOC in a late stage of the disease [25], [26]. According to the limited specificity and sensitivity of CA-125 for EOC in an early stage, other modalities and novel biomarkers are used to increase the accuracy of the test to predict EOC in women. HE4, PRGN and SLPI can be used as well for the detection of EOC [7], [9], [10], [25].

In 1999, Schummer *et al.* reported that HE4 is overexpressed in EOC patients [7]. Following this investigation, HE4 was chosen as a potential tumor marker for EOC in 2003. The mechanism of HE4 in EOC is not yet clear and further research is needed. HE4 is weakly expressed in epithelium cells of reproductive and respirational organs but overexpressed in EOC. Yanaranop and colleagues noted that the specificity of HE4 was 86% and showed that this biomarker in combination with CA-125 is more reliable than CA-125 alone [7], [27].

Carlson and colleagues studied two additional biologically connected serum tumor markers, PGRN and SLPI. PGRN occurs in tumorigenesis and increased tumor invasion. Studies have shown that SLPI expression increases the malignant behavior of cancer cells and in addition, SLPI protects proteins (e.g. PGRN) from serine proteases. Carlson *et al.* concluded that SLPI concentrations are increased in EOC patients and that SLPI exhibits good sensitivity to distinguish early stage EOC from benign cancer [28]. The authors also reported that elevation of PGRN levels is related to a low survival rate. However, the role of both biomarkers in pathogenesis and progression of EOC remains unclear. Further research about the biochemical mechanism of PGRN and SLPI is needed [28].

To summarize, CA-125 is commonly used as biomarker to detect EOC but is not an optimal screening tool due to its low specificity. Therefore, biomarkers with a higher specificity are desired. HE4, PGRN and SLPI are found as predictive biomarkers to detect EOC in an early stage [28]. Diagnostic tools relying on biomarkers will be explained in the next chapter.

### 3 Biosensing

At present, several approaches are being developed to detect and combat cancer, including novel therapeutic approaches, improved tumor imaging and the ultrasensitive monitoring of cancer tumor markers via biosensors. In this regard, enabling early detection is equally important as the discovery of novel and effective anticancer drugs [14]. Currently, diagnostic methods for EOC include TVS, biopsy analysis and tumor marker monitoring. The latter can be done by e.g. enzyme-linked immunosorbent assay (ELISA) and mass spectrometry [4], [5], [14]. Nevertheless, current diagnostic methods not yet common ground given their complexity and cost. As a result, these drawbacks may discourage patients to undergo routine examination. Therefore, early signs of EOC are being overlooked which results in the progression of the cancer and metastasis [14].

Biosensors are appliances that generate signals proportionate to the concentration of an analyte, for example biomarkers in EOC patients' serum, in biological and chemical reactions. The representation of a biosensor setup and associated components are given in Figure 1 [29]. Biosensing is a tool to detect EOC in an early stage and limit the number of progressive cancers. In addition, they are less complicated, cheaper and less invasive than other techniques [4], [5], [14].

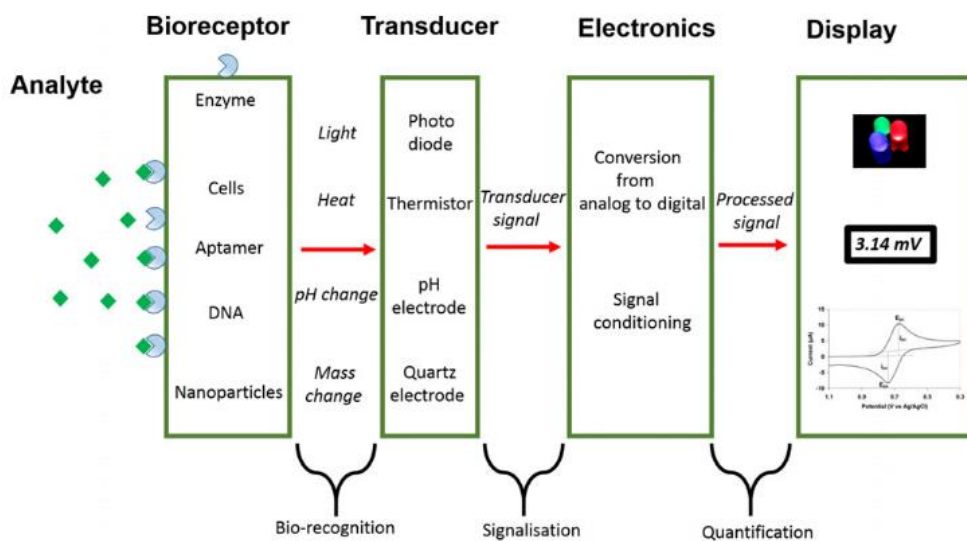


Figure 1: Schematic representation of a biosensor [29, p.2]

As shown in Figure 1, the target molecule (analyte) can bind a bioreceptor. In this thesis, the above-mentioned biomarkers serve as analytes. Biorecognition will result in a measurable signal (e.g. based on light, temperature, pH changes). This signal will be transduced by a so-called transducer, to a digital signal. Finally, a microprocessor converts the transducer signal to a processed signal. Following this, the analyte can be quantified based on an external calibration curve is needed. Biosensing can be used in diagnostic applications for a wide range of cancers, but also in drug discovery and detection of pollutants and micro-organisms as well [29].

In the last decades, several sensitive biosensing methods have been established, among others SPR, ellipsometry and quartz crystal microbalance. SPR is a commonly used method because of its high sensitivity, specificity, low cost and the potential to monitor in real-time. The setup of an SPR device is given in Figure 2. A laser beam is directed through a prism, reflects off a thin gold layer on the prism base and finally hits a detector. At a certain incident angle, which is called the resonance angle ( $\theta$ ), light interacts with the electrons of the gold layer. This induces electron oscillations known as surface plasmons. As a result, an intensity loss in the reflected beam can be observed at this angle  $\theta$  (black line in A, dip in reflected intensity as a function of incident angle Figure 2 B). The surface plasmons are very sensitive to any change at the interface, i.e. variations in the refractive index near the metal layer due to for example biomolecular interactions between analyte and bioreceptor [30], [31].

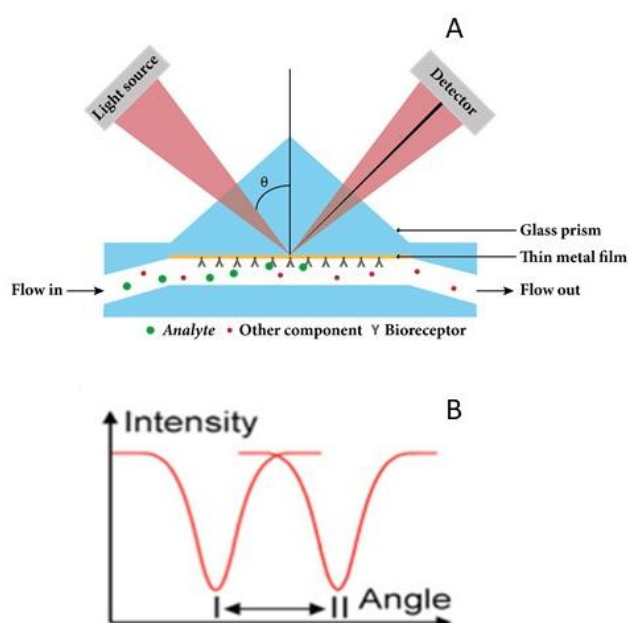


Figure 2: A) The setup of a SPR sensor in the Kretschmann configuration. B) Typical SPR curve with the reflected intensity in function of the incident angle. The curves represent the spectrum of the reflected light before and after refractive index change [30, p.10483]

When the sample with the proper analyte and other components flows through, the analyte will bind the bioreceptor. This biomolecular interaction will induce changes in refractive index and will result in a shift in the observed resonance angle. These changes can be determined by registering the reflected light intensity through a detector. As a result, the analyte concentration can be monitored on a highly sensitive way [30], [31].

As reported in Figure 1, there are several components that can be used as bioreceptors including enzymes and DNA [29]. In addition to these biomolecules, Ta *et al.* reported that antibodies are known as the most commonly applied biomolecules for biosensors [12]. In the next part, a special class of antibodies will be explained as a potential candidate for biosensing purposes [12].

### 3.1 Nanobodies

Antibodies (Abs), also known as immunoglobulins (Igs) are secreted by a special type of white blood cells, namely activated B cell clones or plasma cells. The secreted Igs are naturally occurring proteins that recognize foreign substances, i.e. antigens (Ags) [29], [32]. The binding between antigen and antibody will initiate an immune response in order to destroy the antigen [33]. A full description of immune responses is beyond the scope of this work but can be found in the book 'Kuby Immunology' written by Punt and colleagues [34].

Immunoglobulin- $\gamma$  (IgG) is the most frequent antibody in the blood of mammals. IgGs consist of two pair identical light (L)-chains and heavy (H)-chains. The L-chain contains two polypeptide domains and they are known as the constant and variable domain (abbreviated as CL and VL, respectively). The four H-chain domains are divided in three constant domains (CH1, CH2, CH3) and one variable domain (VH). The structure of an IgG is schematically represented in Figure 3 [1].

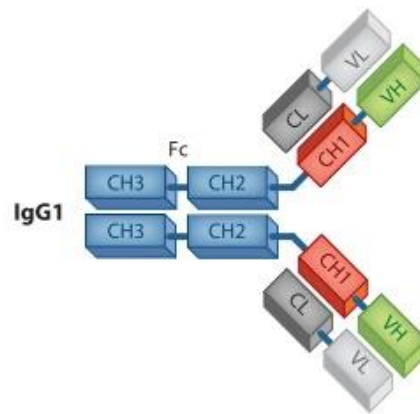


Figure 3: Schematic representation of an IgG antibody [1, p. 777]

A special class of general mammalian IgGs is found in blood of Camelidae. These Igs, also known as heavy-chain antibodies (HCABs), are unique because they lack the L-chain and do not contain CH1. The H-chain of HCABs consists of a dedicated variable domain, referred to as VHH. The function of this VHH in an HCAB is to bind the related Ag and is known to be functionally and structurally equal to the antigen-binding fragment (Fab) of conventional Abs. The range of the single-domain VHH is a few nanometers and therefore, it also known as a nanobody (Nb). A schematic representation of an HCAB and the differences between conventional Abs, HCABs and Nbs is given in Figure 4 [1], [2].

In 2015, Ta *et al.* described Nbs as “powerful next-generation antibodies for therapeutic applications” [12, p.352]. This is because of the advantages over classical Abs, including higher stability, smaller size (diameter ca. 2.5 nm and height ca. 4 nm) and the extended antigen-binding site. Nbs are a tool for therapeutic approaches, but for research and diagnostic applications based on biosensors as well. More specifically, Nbs serve as bioreceptors that are needed to recognize and bind the analyte, e.g. EOC tumor markers [2], [12].

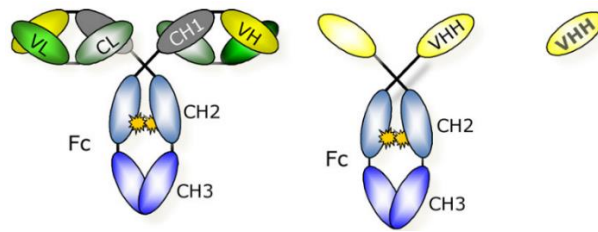


Figure 4: Difference between a conventional Ab (left), an HCAb (middle) and a Nb (right) [2, p.180]

Although Nbs are derived from HCABs found in Camelidae, it is not feasible to extract the HCABs from lama's or camelids in large quantities. Therefore, other procedures are required to produce the Nbs directly. Genetic modification is an ideal tool to produce for example proteins in large amounts in microorganisms. The next part will describe the expression of Nbs through *E. coli*.

### 3.2 Protein expression

Until the emergence of recombinant protein expression, studies based on purified proteins were dependent on the protein's prevalence and stability. Scientists have tried to purify proteins from organisms that contain the highest amount of the desired protein [35], [36]. In the early 1970s, restriction enzymes *HindIII* and *EcoRI* were discovered to cleave DNA into particular fragments at specific sites. This initiated the field of recombinant DNA technology that can be used for the biotechnological expression of proteins. Historically, the first cloning experiments were performed by transferring specific DNA fragments from one bacterial strain to another through a carrier which is called a plasmid<sup>4</sup>. Further cloning experiments followed where a complete bacterial genome was cloned. In addition, researchers discovered that it was possible to clone DNA from different species in other ones. The beginning of the heterologous recombinant gene expression was set [37].

The principle of recombinant DNA technology is represented in Figure 5. The DNA that needs to be cloned is that from the desired expressed protein. In this thesis, it will be the gene of a specific Nb (~ 15 kDa) that binds an EOC biomarker. This can be done by restriction enzymes that cleave both the desired gene and the DNA of the plasmid at the same places, termed restriction sites. Through a technique called ligation, the Nb gene will be joined to the plasmid. This is done by the enzyme DNA ligase. The result is a recombinant plasmid. The plasmid will be transferred into a bacterial cell (*E. coli*) via a process called transformation. This can be done through e.g. heat shock where foreign DNA can be ingested by *E. coli* as a result of pore formation in the cell wall through a sudden increase in temperature [38]. Because of its rapid growth rate, high product yield, cost-effectiveness, and simple scale-up process, *E. coli* is the preferred host for protein expression [35], [38].

In order to be able to express the DNA, the gen can be transcribed as mRNA. The promotor can be seen as the beginning for transcription, since RNA-polymerase will bind it. After this, translation (the process where ribosomes will translate

<sup>4</sup> Circular extrachromosomal DNA

mRNA to proteins) will take place. The whole process is called gene expression. In this thesis, a special mechanism in *E. coli* is used for gene expression, namely the lactose operon (lac operon). The principle is represented in Figure 6. Gene expression will take place if lactose or a derivate, e.g. Isopropyl  $\beta$ -D-1-thiogalactopyranoside (IPTG), is present in the medium of *E. coli*. Lactose or IPTG will bind the lac repressor<sup>5</sup> and will inactivate it. As a result of this, RNA-polymerase becomes active and transcription can start. Thereafter, the proteins encoded by the mRNA are produced by translation at the ribosomes [38].

To ensure only *E. coli* strains with the proper plasmid will be obtained, selectable markers are used. The aim of adding selectable markers stems from the incomplete transformations. It is desirable to recover the *E. coli* clones that own the transferred plasmid. Therefore, a selectable marker like ampicillin resistance is joined to the plasmid. The cells that have the right plasmid will grow on a medium that contains ampicillin (an antibiotic), and the cells that are missing the plasmid will die [38].

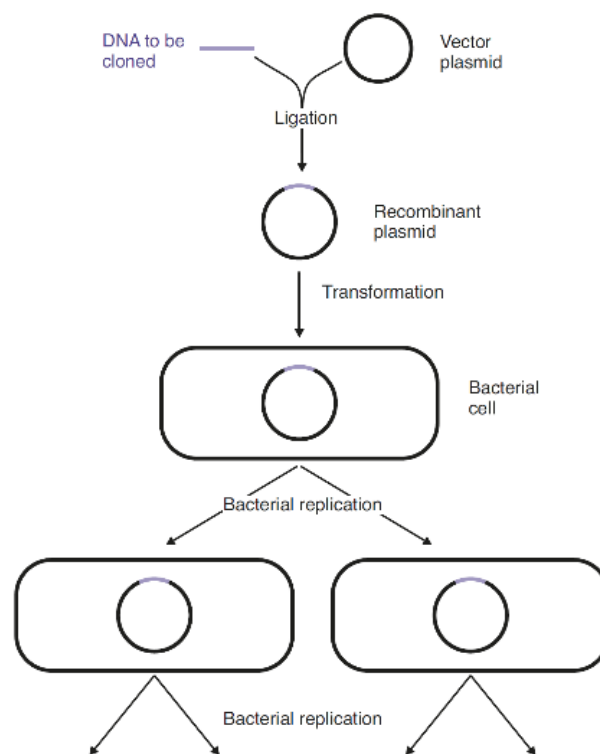


Figure 5: The schematic representation of genetic recombination [38, p. 27]

---

<sup>5</sup> A protein that can bind DNA and inhibit the gene expression

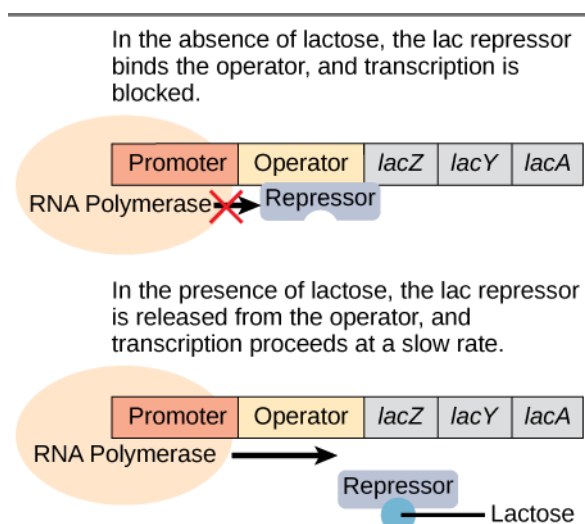


Figure 6: The schematic presentation of the lac operon [39]

Like previously described, the Nb has to be immobilized on a surface in biosensing. The immobilization includes a covalent reaction between two groups *i.e.* one group of the Nb and the other group present on the biosensing surface. Thus, the Nb has to be modified with an extra group through a technique called intein-mediated protein ligation (IPL) [12]. To perform IPL, the Nb has to be expressed with two extra units and is called a fusion protein. The construct of this fusion protein (~42 kDa) in the plasmid pTXB1 is schematically represented in Figure 7. The IPL technique will be described in the next section.

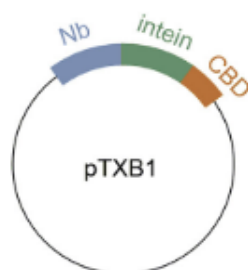


Figure 7: The schematic representation of the fusion protein construct [40, p.30]

### 3.3 Intein-mediated protein ligation

Over the past decade, a lot of research has been done in the field of controlled protein modification. Researchers have recently studied the incorporation of functional groups in a desired protein. For the immobilization of Nbs on a biosensing surface, an alkyne group has to be introduced in the Nb through IPL. This technique is also known as expressed protein ligation (EPL) and was first described by Muir and colleagues [12]. A schematic representation of IPL is given in Figure 8 [12]. Within IPL, the C-terminus of a Nb (protein of interest) is fused to a self-cleavable peptide, called an intein, that contains a thiol (SH) group. In addition, a chitin-binding domain (CBD) is coupled to the Nb-intein entity. The purification of the Nb-intein-CBD fusion protein from other components that are secreted by *E. coli* is done by a chitin column. The fused Nb will be loaded on the column that is filled with chitin resin. The Nb fusion protein will bind the resin via

its CBD, while other components will flow through the column during the washing step. The intein will perform an N-S shift at the terminus of the Nb to form a thioester intermediate, which make it susceptible to nucleophiles. In the next step, a molecule with a thiol function will be added to the column in order to react with the thioester carbonyl from the Nb. This process is called native chemical ligation. The Nb will be cleaved from the intein. The formed molecule is unstable and will undergo an S-N shift, to form a more stable amide bond. The end product is depended on the added thiol-containing molecule. This can be for example dithiothreitol (DTT) or a cysteine-alkyne based linker. A primary nucleophile, 2-mercaptoethanesulfonic acid (MESNA), is usually added to increase the efficiency of the modification. A thioester intermediate is formed which can subsequently undergo a second nucleophilic attack by DTT or the linker. The end product of IPL is a wild-type protein (the Nb itself) when DTT is added, while by adding the cysteine-alkyne based linker, an alkynated protein will be formed. When considering biosensing purposes, a cysteine-alkyne linker is the desired molecule. The introduced alkyne function is available to react with a second group for example an azide function present in the biosensor surface [12].

Like previously described, the aim of using Nbs in diagnostic tools is to detect specific biomarkers in the blood of EOC patients. The Nb with its alkyne function has to be immobilized on the biosensor surface. This immobilization has to be site-specific and covalently oriented in order for the biomarker to bind. To provide the site-specific, covalent immobilization, the so-called 'click' reactions are performed. They were first described in 2001 by Kolb and colleagues and can be defined as a set of selective and efficient organic, chemical reactions. Since then, a lot of 'click' reactions have been described, including Michael addition, Diels-Alder and the copper-catalyzed azide-alkyne cycloaddition (CuAAC). The latter, also known as the copper-catalyzed Huisgen 1,3-dipolar cycloaddition, is the most used and is represented in Figure 9. In this figure,  $R^1$  is the biosensor surface,  $R^2$  is the Nb and  $R^3$  an H-atom. The alkyne function at the terminus of the modified Nb can react with the azide ( $N_3$ ) group, present in a biosensor surface. The result is a 1,2,3-triazole, first synthesized in 1893 by A. Michael. The reaction can be performed under mild reaction conditions with a minimal of byproducts. Many Cu(I) sources are available to be used as catalysts but mostly, the catalyst is prepared by the reduction of Cu(II) salts Nb [11], [13] [40].



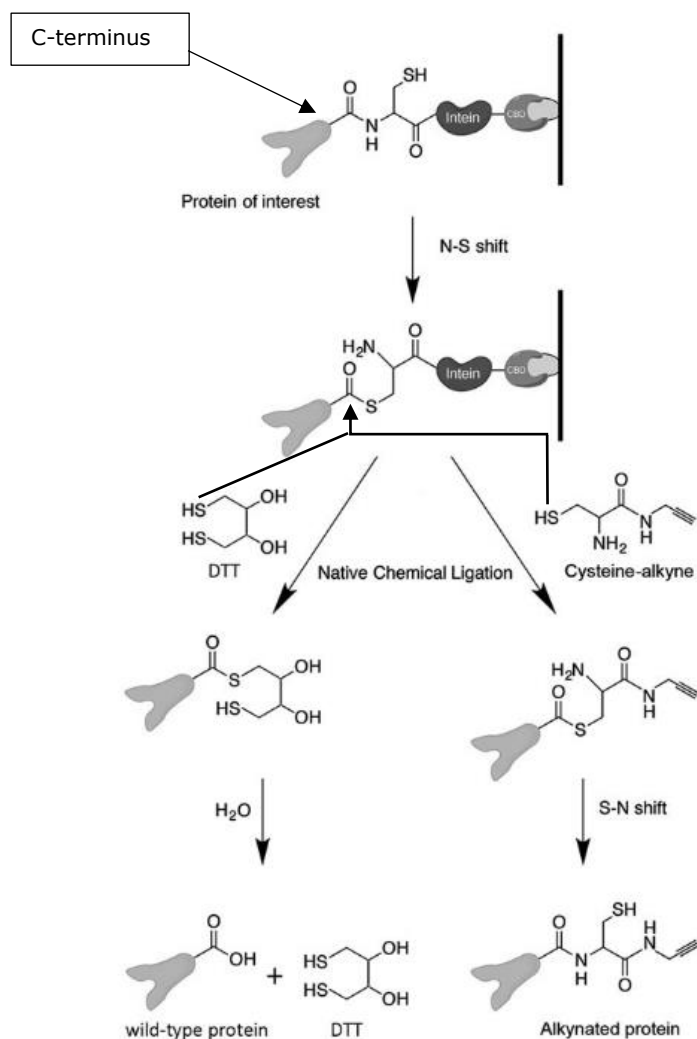


Figure 8: The IPL mechanism, adapted from [12, p.352]

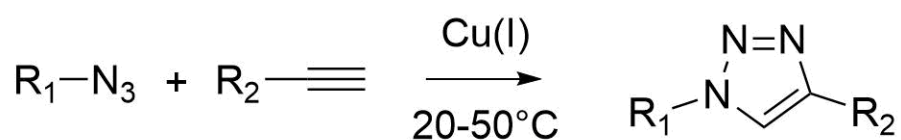


Figure 9: The copper(I)-catalyzed azide/alkyne cycloaddition (CuAAC), adapted from [41]

Based on previous literature study, present work will focus on the expression of the proper fusion protein in 3 different strains of *E. coli*. This will be followed by the purification to obtain the wild the Nb itself. In the end, the experimental results will be evaluated through SDS-PAGE and a conclusion will be made.

## 4 Material and methods

All chemicals and reagents were obtained from Sigma-Aldrich unless stated in Table 3.

Table 3: The obtained chemicals and reagents, other from Sigma-Aldrich

<b>Acros Organics</b>	Ammonium sulphate, anhydrous magnesium sulphate, glucose, N-hydroxysuccinimide (NHS), N, N-dimethylformamide (DMF), sodium phosphate dibasic, yeast extract
<b>Becton Dickinson and company</b>	Bacto-agar, bacto-tryptone
<b>VWR Chemicals</b>	Acetic acid, IPTG, methanol, sodium chloride, tetrahydrofuran (THF)
<b>PB Perbio</b>	Coomassie blue
<b>Amresco</b>	Ampicillin, glycerol
<b>TCI Europe</b>	Di-tert-butyl-dicarbonate, 1-(3-Dimethylaminopropyl)-3-ethylcarbodiimide hydrochloride (EDC), L-cysteine
<b>FluoroChem</b>	Propargylamine
<b>Millipore</b>	Milli-Q grade water
<b>Thermo Fisher Scientific</b>	B-PER (bacterial protein extraction reagent), HEPES (4-(2-hydroxyethyl)-1-piperazineethanesulfonic acid)
<b>New England Biolabs</b>	Chitin slurry
<b>Spectrum laboratories</b>	Molecular porous membrane tubing
<b>Biotage</b>	Solid phase extraction (SPE) columns, frits

### 4.1 Preparation of the agar plates and media

This part will describe the preparation of the Luria-Bertani (LB) agar plates and the different growth media used for the expression of the fusion protein Nb-intein-CBD in *E. coli*. Three strains of *E. coli* (2210, 3237, 2276) were used, at which each strain carried the individual Nb-gene for HE4 (2210), SLPI (2276) and PRGN (3237).

#### **Luria-Bertani medium**

The LB medium was prepared by dissolving 10 g/l bacto-tryptone, 5 g/l yeast extract and 10 g/l NaCl in 1 l distilled water (Milli-Q). Thereafter, the culture media was divided into culture flasks and subsequently autoclaved at 120°C for 20 min at 15 psi.

For the preparation of the LB agar plates, LB medium was prepared and 15 g/l agar was added before autoclaving at 120 °C for 20 min at 15 psi. The mixture was allowed to cool to 50 °C and at this temperature, 100 µg/ml ampicillin was added. Thereafter, the content was divided in Petri dishes and left to cool down for 30 min at room temperature. After this, the plates were turned upside down for 20 min and finally, they were wrapped with parafilm and stored at 4 °C until use.

### Terrific broth medium

The terrific broth (TB) medium was prepared by two separate mixtures. Mixture A consists of 24 g/l yeast extract and 12 g/l bacto-tryptone in Milli-Q water. Thereafter, 0.004% glycerol was added to the mixture. For mixture B, 0.72 M K<sub>2</sub>HPO<sub>4</sub> and 0.17 M KH<sub>2</sub>PO<sub>4</sub> were dissolved in a separate flask. Mixture A and B were autoclaved at 120 °C for 20 min at 15 psi. Finally, both mixtures A and B were added together with a volume ratio (ml) of 9:1 and 0.1% of sterile glucose was added.

### Tryptone yeast peptone medium

For the preparation of the tryptone yeast peptone (TYP) medium, 0.3 % yeast extract, 0.3 % bacto-tryptone, 25 mM (NH<sub>4</sub>)<sub>2</sub>SO<sub>4</sub>, 2 mM MgSO<sub>4</sub>, 0.2 % glycerol, 0.01 % glucose, 0.05 % lactose, 50 mM Na<sub>2</sub>HPO<sub>4</sub> and 50 mM KH<sub>2</sub>PO<sub>4</sub> were dissolved separately in a falcon tube. Thereafter, they were autoclaved at 120 °C for 20 min at 15 psi. The tubes with glucose and lactose were sterilized using a 0.2 µm syringe filter.

## 4.2 Parameter-dependent protein expression

In this part, the methods for the fusion protein expression optimization in *E. coli* will be described. The varied expression parameters are based on the results in the article of Ta and colleagues [12]. They reported a similar study about an efficient protocol of protein expression, but with a nanobody that targets vascular cell adhesion molecule 1. In this work, four parameters of the expression are varied and are given in Table 4.

Table 4: The varied expression parameters

Temperature <i>T</i> (°C)	Medium <i>M</i>	Concentration IPTG <i>C</i> (mM)	Time <i>t</i> (hours)
28 - 37	LB - TB - TYP	0.1 - 0.5 - 1	0 - 1 - 2 - 3

One single colony of each *E. coli* strain was taken from the inoculated agar plate with a pipet tip. The tip was placed in a test tube that contained 5 ml **M** medium and 0.1 mg/ml of ampicillin was added. The tubes with *E. coli* were put overnight in an (IKA KS4000i control) shaking incubator at 37°C and 220 rpm. The next day, 1 ml of each preculture was put in flasks that contain 50 ml of LB medium and 0.1 mg/ml of ampicillin. The flasks were put in the shaking incubator at 37 °C and 220 rpm. The absorbance value was measured after 3 hours with an Amersham Biosciences Ultrospec 10 spectrophotometer. Once the value reached 0.6-0.8,

IPTG with **C** mM was added to the flasks. The flasks were incubated in a shaking incubator at **T** °C for **t** hours at 220 rpm. After this, 100 µl was taken from each expression flask and put in an Eppendorf tube. The samples were centrifuged (Eppendorf 5415R centrifuge) for 5 min at 16200 rpm and 15 °C. In the end, the supernatant was removed and the pellet was stored at 4°C. The remaining culture was centrifuged (Eppendorf 5804R centrifuge) for 10 min at 5000 rpm and 15 °C. The supernatant was removed and the cell pellet was stored at -20 °C.

### 4.3 SDS-PAGE

SDS-PAGE was performed to assess protein composition by separating the proteins based on their size. The technique was first described by Laemmli and is used to evaluate purifications and determine the molecular weights of proteins [42].

For the SDS-PAGE, a Bio-RAD Mini-Protean Tetra cell was used. First of all, the separating gel was made of 0.375 M TRIS-Cl pH 8.8, 15 % acrylamide 0.8 % bis, 0.1 % sodium dodecyl sulphate (SDS), 0.007 % ammonium persulfate (APS) and 0.01 % tetramethylethylenediamine (TEMED). The stacking gel was prepared using 0.625 M TRIS-Cl pH 6.8, 0.05 % acrylamide 0.8 % bis, 0.01 % SDS, 0.005 % APS and 0.0016 % TEMED. The separating gel was first poured in the gel holders. After polymerization, the stacking gel was added. The stored samples from the expression were prepared by adding gel loading buffer (GLB) and put in a boiling water bath for 10 min. The preparation of GLB was done by using 100 mM TRIS-Cl pH 6.8, 4 % SDS, 0.002% Bromophenol blue, 20 % glycerol and 10 % 2-mercaptoethanol. Thereafter, the samples were centrifuged (Eppendorf 5415R centrifuge) for 4 min at 16200 rpm and 15 °C. Afterwards, the samples were loaded onto the stacking gels as well as a Thermo Scientific protein ladder (Page Ruler Plus 26619). The gel electrophoresis was set for 90 min at 100V. After running, the gels were stained with staining buffer (Expedeon Instant Blue) for 20 min. In the end, the gels were cleaned a couple of times with water.

### 4.4 Purification

The expressions of the fusion protein before purification were performed following the optimal expression parameter settings. The varied purification parameters are based on the standard protocol settings of the Impact kit [43]. This protocol is made for the purification of the expressed maltose-binding protein in *E. coli*, but is similar to the purification that is needed for the nanobodies in this work. The principle of the purification SDS-PAGE gels is represented in Figure 10. Only the loading of lane 1, 5, 6, 7, 8, 9 and 10 is performed in this work and will be discussed. Lane 5 (flow through 1) is meant to determine the binding efficiency of the fusion protein on the chitin resin and a weak intensity band is desirable. Other proteins may be present as well. The washing step is presented in lane 6 and is meant to check if no other proteins were left behind in the column. A small amount of fusion protein is acceptable. Lane 7 (+ cleavage reagent DTT) is in this work represented as flow through 2 and a small amount of fusion protein and purified Nb is acceptable. Elution 1 and 2 are represented in lane 8 and 9, respectively. After cleavage with DTT, a high intensity band at the purified Nb is desirable, the presence of fusion protein is not acceptable. When the chitin resin (bead) is

checked on the gels (lane 10), a high intensity band at the intein-CBD is desirable, which means the cleavage is successfully completed.

*Note: in this work, a different order of loading is performed and can be seen on the gels that have been added to the appendices.*

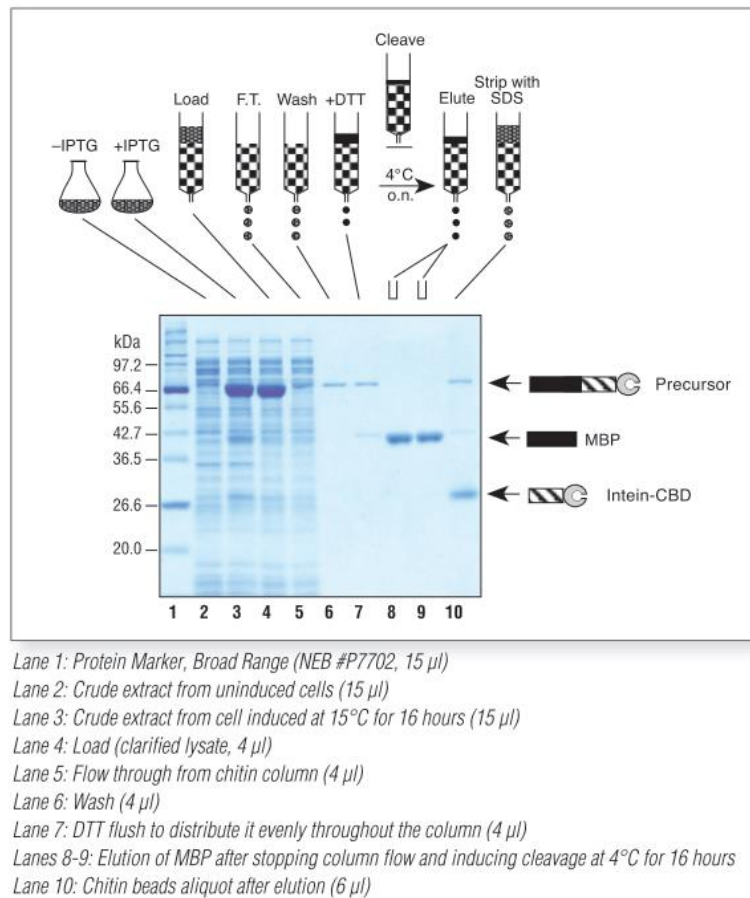


Figure 10: The principle of the SDS-PAGE result of the Nb purification after fusion protein expression in *E. coli*, adapted from [43, p. 5]

## Protein extraction

Before purification of the expressed nanobodies, protein extraction was needed to separate proteins from other cell components. The cell pellet from 300 ml bacterial culture in a falcon tube was resuspended in 6 ml B-PER supplemented with DNase I<sup>6</sup> by pipetting up and down. The falcon tube was incubated for 15 min at room temperature. Next, the content was centrifugated for 30 min at 14000 rpm and 4 °C. In the end, the supernatant was collected for purification.

<sup>6</sup> DNase I is an enzyme that degrades the present DNA

## Purification

In this part, the methods for the Nb purification optimization will be described. Two parameters of the expression are varied and are given in Table 5.

Table 5: The varied purification parameters

<b>Cleavage time <i>Ct</i> (hours)</b>	<b>Cleavage temperature <i>CT</i> (°C)</b>
16 - 40	4 - Room temperature

First of all, the filter frits of two empty solid phase extraction (SPE) columns were pre-wetted with Milli-Q water. Secondly, 3 ml of chitin was added to each column and was equilibrated by gravity. Next, the column buffer (CB) was prepared by dissolving 4.766g HEPES, 29.22g NaCl and 0.2922g EDTA in 1l Milli-Q water. Each column was washed with 10 column volumes of Milli-Q water and subsequently 10 column volumes of column buffer. Thereafter, the cell lysate from protein extraction was divided in two portions and each portion was loaded on a chitin column. The flow-through (FT1) was collected and stored at 4°C. To continue, each column was washed with 20-30 column volumes of CB. The washing flow-through (W1 and W2) was collected and stored at 4°C. Column 1 was quickly flushed with 3 ml of CB (negative control) and also column 2 was quickly flushed but with 3 ml of freshly prepared cleavage buffer (30 mM DTT in CB). Both flow-throughs (FT2) were collected and stored at 4°C. The SPE columns were closed by putting a stopper on the exit. Thereafter, 1 column volume of the previously selected cleavage buffer was added to each column and incubated for ***Ct*** hours at ***CT*** °C. Both columns were eluted with 1.5 column volumes of CB while collecting the elution samples (El 1 and El2) in falcon tubes. Next, the collected elution samples had to be purified through dialysis. The samples were loaded in a molecular porous membrane tubing and were placed in a beaker with PBS buffer, pH 7.4. The buffer was changed 3 times at 2-hour intervals. The elution samples from column 1 (CB) were captured in falcon tubes. The elution samples from column 2 (DTT), containing now the nanobodies that were purified from other components, were captured in a falcon tube. Finally, all falcon tubes were stored at 4°C.

### 4.5 Nanodrop

The concentration measurements of the Nbs were done via a spectrophotometer (Nanodrop ND-1000). First of all, 2 µl RNA-polymerase was pipetted onto the pedestal. The arm was closed and was moved up and down several times to clean the Nanodrop. After this, the pedestal was wiped clean with a tissue. To continue, 2 µl PBS was pipetted onto the pedestal, the arm was closed and measurement was performed as blank. Thereafter, 2 µl Nb sample (from CB or DTT elution) was pipetted onto the pedestal, the arm was closed and the concentration of protein was measured relative to the blank. Finally, the device was cleaned in the same way as previously mentioned.



## 5 Results and discussion

This chapter will discuss the SDS-PAGE results of the experiments that were performed as described in materials and methods.

### 5.1 Parameter-dependent fusion protein expression

In this part, the results of the parameter-dependent experiments will be discussed.

#### Temperature

The results of the temperature-dependent fusion protein expression on SDS-PAGE are shown in Figure 11. There is a band visible between 35-55 kDa, which means the fusion protein ( $\sim 42$  kDa) was present in the sample. The color of the bands of 37 °C for all three strains of *E. coli* is more intensive than those of 28 °C, which means that the expression was increased at 37 °C. In this thesis, 37 °C is the optimal temperature for protein expression. Baeshen *et al.* reported that growth of *E. coli* at lower temperatures leads to decreases in protein synthesis rates. Schein and colleagues noted that growth of *E. coli* at 37 °C can cause some inclusion bodies and lower temperatures at prolonged time can be optimal for protein expression [35], [44]. Inclusion bodies (highly aggregated proteins) are non-active products as a result of the high-level expression of recombinant proteins [45]. The presence of these aggregates in cells can be observed through phase contrast microscopy or after expression via SDS-PAGE but both were not performed in this work [45], [46]. As a result of this, all following parameter-dependent experiments were performed at 37 °C. To declare the difference in protein expression between the three strains, a 3D-model of the protein's structure and amino acid sequence needs to be observed. The examination of the 3D-model is beyond the scope of this work and future research is recommended.

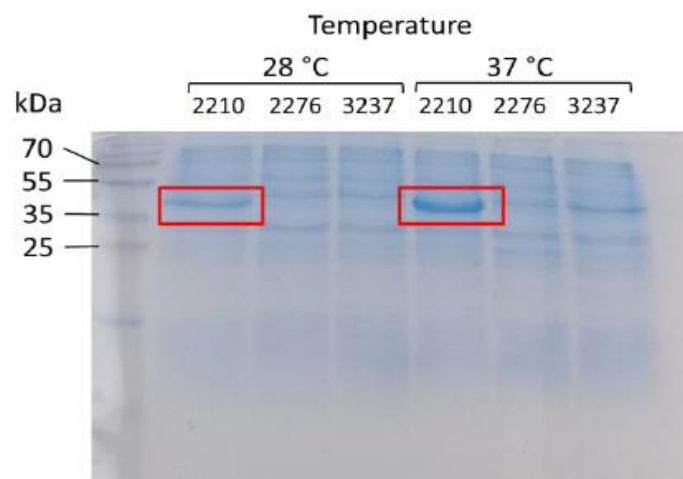


Figure 11: Temperature-dependent fusion protein expression for strains 2210, 2276 and 3237 at 28°C and 37°C. The other 3 parameter settings were chosen at random (1mM, LB, 3hours). The red rectangles show that the expression for strain 2210 is the highest in contrast to the other strains



## IPTG concentration

Figure 12 shows the results of the IPTG concentration-dependent fusion protein expression on SDS-PAGE. For strains 3237 and 2210, the bands between 35-55 kDa are more intensive at 0.1 mM IPTG than at the other concentrations. This means that the expression of the fusion protein for both strains is the highest when 0.1 mM IPTG is added. For strain 2276, no clear effect of the different concentrations is visible. It can be concluded that the concentration of IPTG has an influence on protein expression. Wang and colleagues reported that higher amounts of IPTG leads to overexpression. This will affect the folding of proteins and as a result of this, protein aggregates will be formed and the desired fusion protein will not be produced in high yield [47]. For strain 2276, no concentration-dependent conclusions can be made. As a result of this, the following time- and medium-dependent experiments were performed at 37°C and with a concentration of 0.1 mM IPTG.

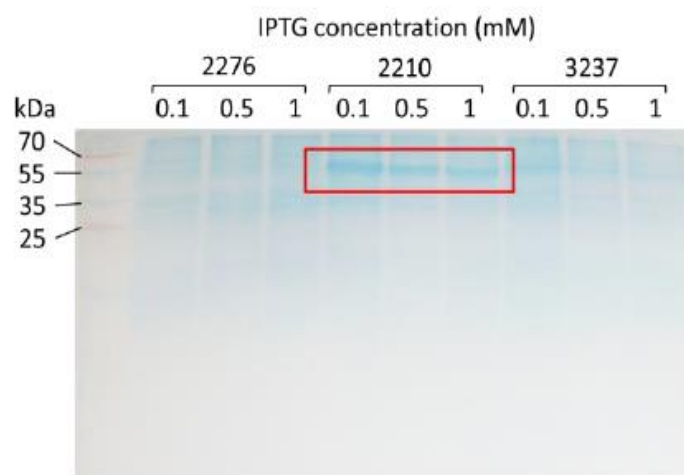


Figure 12: IPTG concentration-dependent fusion protein expression for strains 2276, 2210 and 3237 at 37°C with 0.1 mM, 0.5 mM and 1 mM. The other 2 parameter settings were chosen at random (LB, 3hours). The red rectangles show that the expression for strain 2210 is the highest in contrast to the other strains

## Time

Figure 13 shows the results of the time-dependent fusion protein expression on SDS-PAGE for the three strains. As it can be seen in A and C, the intensity of the band between 35-55 kDa rises with increasing time for strains 2210 and 3237, respectively. The highest amount of expression for strains 2210 and 3237 was after 2 to 3 hours. For strain 2276, no conclusions can be made based on the weak bands of the SDS-PAGE (B). SDS-PAGE is also done for samples with no IPTG to compare if there is a difference in band intensity with 0 hours. As can be seen in Figure 13, there is no visible difference in intensity between -IPTG and 0 hours. For the results of strain 2210 and 3732, reference is made to the article of Wang and colleagues [47]. They reported that the enzyme activity will stay constant, but the yield of the product will increase with longer times. Because of this, the bands for strain 2210 and 3732 on SDS-PAGE have a higher intensity at longer times than when shorter times are chosen. As a result of this, the last medium-dependent experiments were performed at 37°C, with a concentration of 0.1 mM IPTG and for 2-3 hours.

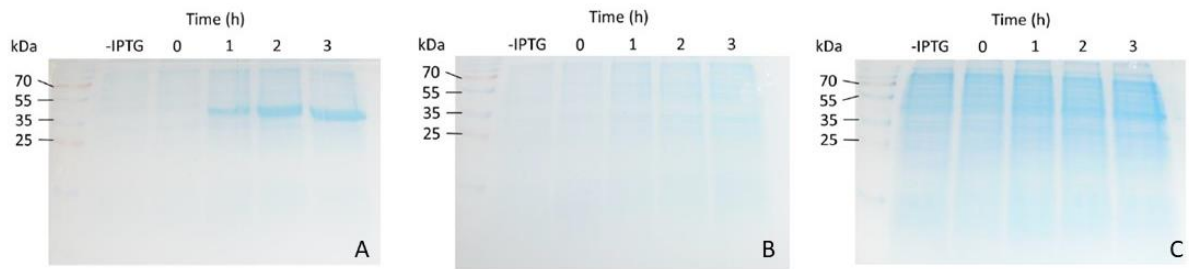


Figure 13: Time-dependent fusion protein expression **A**: Strain 2210 at 37°C, with 0.1mM and for 0, 1, 2 and 3 hours. SDS-PAGE is also done for sample with no IPTG. **B**: Strain 2276 at 37°C, with 0.1mM and for 0, 1, 2 and 3 hours. SDS-PAGE is also done for sample with no IPTG. **C**: Strain 3237 at 37°C, with 0.1mM and for 0, 1, 2 and 3 hours. The other parameter setting was chosen at random (LB).

## Medium

The results of the medium-dependent fusion protein expression on SDS-PAGE are shown in Figure 14. For strain 3237 and 2276, no conclusions can be made based on the weak bands of the SDS-PAGE. For strain 2210, the LB and TB medium have the highest expression of fusion protein, based on the intensity of the band color. This is in contrast to the TYP medium that has the lowest expression, based on the intensity of the band color. LB is the most used medium because it permits rapid growth and high yields [48]. In addition, TB is a richer medium and includes an extra energy source, namely glycerol. This leads to faster growth and therefore, also even higher yields can be achieved. TB is usually used for growing larger cultures [49]. TYP medium is a subtype of NZ-Amine A Yeast Peptone (ZYP) medium where the NZ-Amine A was replaced by tryptone. TYP is a very rich source of amino acids and peptides that is necessary for growth [50]. As a result of the high amount of these compounds, *E. coli* will grow faster and a higher yield is expected. Nevertheless, it is expected that all nutrients are consumed for cell growth when expression would have started. As a result of this, lower expression level will be observed. Because of this, lower intensity of the bands can be observed on the TYP SDS-PAGE gels.

*Note: for the TYP medium, adding of IPTG was not implemented since this medium contains lactose that will induce protein expression.*

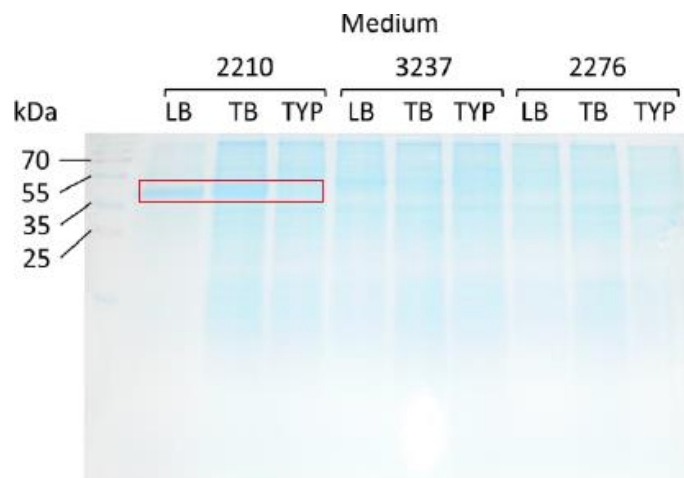


Figure 14: Medium-dependent fusion protein expression for strain 2210, 3237 and 2276 at 37°C, with 0.1mM, for 2-3 hours and with LB, TB and TYP medium. The red rectangles show that the expression for strain 2210 is the highest in contrast to the other strains.

## Optimal settings

The SDS-PAGE result of the optimal settings experiment is given in Figure 15. The expression is done at 37 °C with 0.1 mM IPTG for 2.5 hours. Both LB and TB media are tested. For strain 2210, a high intensity band is visible between 35 and 55 kDa for both media. Strain 3237 gives a lower intensity band between 35 and 55 kDa, in contrast to strain 2210. For strain 2276, no conclusions can be made since the intensity of the band between 35 and 55 kDa is too weak.

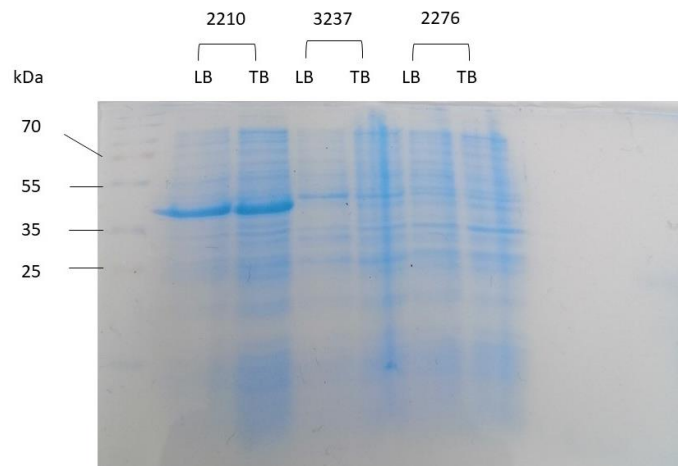


Figure 15: Fusion protein expression with the optimal parameter settings for strains 2210, 3732 and 2276

## 5.2 Purification

In this part, the results of the purification experiments will be discussed. The first purification experiment was performed following the standard protocol settings of the Impact kit for maltose binding protein. The second and third purification experiments are performed with varying cleavage time and temperature [43].

### First purification experiment

This purification experiment was performed for the Nbs derived from all three strains of *E. coli*. Following the standard protocol settings, the cleavage temperature was set at 4°C and the cleavage time was 16 hours. The SDS-PAGE results have been added to Appendix A: Results of the first purification experiment. The bands have a weak intensity and may be due to a too large sample volume [51]. As result of this, no reliable conclusions can be made.

### Second purification experiment

The second purification experiment was performed for the Nb derived from *E. coli* strain 2276. The used settings were 4°C for cleavage temperature and 40 hours for cleavage time. The SDS-PAGE results of have been added to Appendix B: Results of the second purification experiment. Similar to previous results, the bands have a weak intensity and may be due to a too large sample volume [51]. As result of this, no reliable conclusions can be made.

### **Third purification experiment**

The last purification experiment was performed for the Nbs derived from all three strains of *E. coli*. This experiment was done at room temperature (cleavage temperature) and a cleavage time of 16 hours was set. The SDS-PAGE results have been added to Appendix C: Results of the third purification experiment. As can be seen in lane FT1 on all gels, a high intensity band is observed around 15 kDa. This is probably the single Nb (~15 kDa) and is expected to be absent in FT1 [43]. This means that the Nb has been released before adding the cleavage reagent. The reason of that might be due to a too long storage time of the expressed proteins and experiments needs to be repeated for clearer results. In addition, gel D contains a lot of smear as a result of an unsuccessful gel development. The possible cause of this may be that the protein sample is not fully denatured [51]. As a result of previous descriptions, no reliable conclusions can be made.

### **5.3 Nanodrop**

The results of the Nb concentration measurements will be discussed in this part. The measurements through Nanodrop are performed after the three purifications that were discussed in the previous part.

The results of the concentration measurements were put in a bar chart and have been added to Appendix A: Results of the first purification experiment, Appendix B: Results of the second purification experiment, Appendix C: Results of the third purification experiment. The DTT bars are the concentration measurements of the elution samples with the purified Nbs. The blanco bars represent the negative controls. As can be seen on the charts, the concentration of the Nbs is very low in each sample. In addition, the negative controls have a certain concentration, while this is not expected, due to the low concentrations. Therefore, reliable conclusion of the concentration measurements cannot be made.



## 6 Conclusion

The aim of this thesis was to optimize the biotechnological production of nanobodies in *E. coli* to be used in diagnostic tools for EOC. In this thesis, the Nbs were expressed together with the intein-CBD entity (referred to as fusion proteins) in order to perform the IPL technique. The end product was the wild-type protein (Nb). First, the optimization of four expression parameters was performed, namely temperature, medium, time and concentration of the inducer. Secondly, the purification of the Nbs on a chitin column was studied. The results were evaluated on SDS-PAGE and in the end, concentration measurements were performed.

The optimization of the expression parameters was successfully completed. The optimal expression settings are given in Table 6. Although for time and medium, it cannot be clearly concluded which settings are the best, based on the SDS-PAGE results. About the medium, both LB and TB give a high intensity and thus a high expression level. The optimal expression time lies between 2 and 3 hours.

Table 6: The optimal parameter settings for protein expression

<b>Temperature (°C)</b>	<b>Medium</b>	<b>Concentration IPTG (mM)</b>	<b>Time (hours)</b>
37	LB - TB	0.1	2 - 3

For the purification optimization and concentration measurement of the Nbs, no reliable results were obtained and therefore, no conclusion can be made.

### Future perspectives

It is suggested to do further experimental work on the results of this work, since the SDS-PAGE gels and concentration measurements are not reliable. The gels were unclear and this could have been a result of older reagents or a too large sample volume. The concentration measurements can also be performed by the 'Bradford protein assay' which gives a more accurate result than the technique that is used in this work.

It would be interesting to test the influence of other parameters on protein expression. For example, only 28 and 37 °C are tested for the optimal setting and maybe values a little lower and higher than 37 °C can be examined. The same applies to concentration and time. Another medium can also be tested but further research is needed.

It is also possible to perform IPL to modify the Nbs with an alkyne function. The results on SDS-PAGE and the concentration may be different so it would be interesting to perform IPL in combination with a cysteine-alkyne based linker.

Concerning the purification, other parameters can be investigated as well. To increase the binding of the fusion protein on the chitin column, the volume of chitin resin can be increased. To obtain more purified Nb in the elution fraction, the concentration of DTT can be adjusted.

The development of a biosensor with multiple nanobodies is another challenge for researchers to examine. With this concept, different biomarkers can be detected at the same time and an accurate diagnosis can be made.

## References

- [1] S. Muyldermans, "Nanobodies: Natural Single-Domain Antibodies," *Annu. Rev. Biochem.*, vol. 82, no. 1, pp. 775–797, 2013.
- [2] E. De Genst *et al.*, "Camelid immunoglobulins and nanobody technology," *Vet. Immunol. Immunopathol.*, vol. 128, no. 1–3, pp. 178–183, 2008.
- [3] The World Ovarian Cancer Coalition, "The World Ovarian Cancer Coalition Atlas: Global Trends in Incidence, Mortality and Survival," *The every woman study*, no. April, pp. 1–39, 2018.
- [4] G. C. Jayson, E. C. Kohn, H. C. Kitchener, and J. A. Ledermann, "Ovarian cancer," *Clin. Obstet. Gynecol.*, vol. 384, pp. 1376–1388, 2014.
- [5] B. T. Hennessy, R. L. Coleman, and M. Markman, "Ovarian cancer," *Curr. Obstet. Gynaecol.*, vol. 374, pp. 1371–1382, 2009.
- [6] U. L. Günther, "Metabolomics Biomarkers for Breast Cancer," *Pathobiology*, vol. 82, no. 3–4, pp. 153–165, 2015.
- [7] R. Lu, X. Sun, R. Xiao, L. Zhou, X. Gao, and L. Guo, "Human epididymis protein 4 (HE4) plays a key role in ovarian cancer cell adhesion and motility," *Biochem. Biophys. Res. Commun.*, vol. 419, no. 2, pp. 274–280, 2012.
- [8] R. Molina *et al.*, "HE4 a novel tumour marker for ovarian cancer: comparison with CA 125 and ROMA algorithm in patients with gynaecological diseases.," *Tumour Biol.*, vol. 32, no. 6, pp. 1087–1095, 2011.
- [9] S. M. Steinberg, N. Houston, E. C. Kohn, M. Yu, and J. J. Han, "Progranulin is a potential prognostic biomarker in advanced epithelial ovarian cancers," *Gynecol. Oncol.*, vol. 120, no. 1, pp. 5–10, 2011.
- [10] S. Tsukishiro, N. Suzumori, H. Nishikawa, A. Arakawa, and K. Suzumori, "Use of serum secretory leukocyte protease inhibitor levels in patients to improve specificity of ovarian cancer diagnosis," *Gynecol. Oncol.*, vol. 96, no. 2, pp. 516–519, 2004.
- [11] D. T. Ta *et al.*, "Enhanced biosensor platforms for detecting the atherosclerotic biomarker VCAM1 based on bioconjugation with uniformly oriented VCAM1-targeting nanobodies," *Biosensors*, vol. 6, no. 3, pp. 1–17, 2016.
- [12] D. T. Ta *et al.*, "An efficient protocol towards site-specifically clickable nanobodies in high yield: Cytoplasmic expression in *Escherichia coli* combined with intein-mediated protein ligation," *Protein Eng. Des. Sel.*, vol. 28, no. 10, pp. 351–363, 2015.
- [13] E. Steen Redeker, D. T. Ta, D. Cortens, B. Billen, W. Guedens, and P. Adriaensens, "Protein engineering for directed immobilization," *Bioconjug. Chem.*, vol. 24, no. 11, pp. 1761–1777, 2013.
- [14] R. Ranjan, E. N. Esimbekova, and V. A. Kratasyuk, "Rapid biosensing tools for cancer biomarkers," *Biosens. Bioelectron.*, vol. 87, no. September 2016, pp. 918–930, 2017.
- [15] National Health Service, "Ovarian Cancer," *CDC*, 2019. [Online]. Available: <https://www.nhs.uk/conditions/ovarian-cancer/>. [Accessed: 25-Mar-2019].
- [16] P. T. Kroeger and R. Drapkin, "Pathogenesis and heterogeneity of ovarian



- cancer," *Current Opinion in Obstetrics and Gynecology*, vol. 29, no. 1. pp. 26–34, 2017.
- [17] J. Prat, "Staging Classification for Cancer of the Ovary, Fallopian Tube, and Peritoneum," *Obstetrics and Gynecology*, vol. 124, no. 1. International Federation of Gynecology and Obstetrics, pp. 1–5, 2014.
- [18] A. Stephen and M. D. Cannistra, "Cancer of the Ovary," *N. Engl. J. Med.*, vol. 351, pp. 2519–2529, 2013.
- [19] E. A. Eisenhauer, "Real-world evidence in the treatment of ovarian cancer," *Ann. Oncol.*, vol. 28, no. 8, pp. 61–65, 2017.
- [20] S. Lheureux, C. Gourley, I. Vergote, and A. M. Oza, "Epithelial Ovarian Cancer," *Dewhurst's Textb. Obstet. Gynaecol. Eighth Ed.*, vol. 393, pp. 1240–1253, 2019.
- [21] K. Selwood, "Side Effects of Chemotherapy," in *Cancer in Children and Young People: Acute Nursing Care*, F. Gibson and L. Soanes, Eds. John Wiley & Sons, 2008, pp. 35–71.
- [22] E. Houben *et al.*, "Chemotherapy for ovarian cancer in the Netherlands: a population-based study on treatment patterns and outcomes," *Med. Oncol.*, vol. 34, no. 4, pp. 1–13, 2017.
- [23] J. Marcin, "What Is a Transvaginal Ultrasound?," 2017. [Online]. Available: <https://www.healthline.com/health/transvaginal-ultrasound>. [Accessed: 28-Mar-2019].
- [24] P. Bottoni and R. Scatena, "The Role of CA 125 as Tumor Marker: Biochemical and Clinical Aspects," in *Advances in Cancer Biomarkers*, vol. 867, Rome: Springer Science+Business Media Dordrecht, 2015, pp. 229–244.
- [25] R. G. Moore, S. MacLaughlan, and R. C. Bast, "Current state of biomarker development for clinical application in epithelial ovarian cancer," *Gynecol. Oncol.*, vol. 116, no. 2, pp. 240–245, 2010.
- [26] N. Urban, M. W. Mcintosh, M. R. Andersen, and B. Y. Karlan, "Ovarian cancer screening," vol. 17, pp. 989–1005, 2003.
- [27] V. Dochez, H. Caillon, E. Vaucel, J. Dimet, N. Winer, and G. Ducarme, "Biomarkers and algorithms for diagnosis of ovarian cancer: CA125, HE4, RMI and ROMA, a review," *J. Ovarian Res.*, vol. 7, pp. 1–9, 2019.
- [28] A. M. Carlson *et al.*, "Utility of Progranulin and Serum Leukocyte Protease Inhibitor as Diagnostic and Prognostic Biomarkers in Ovarian Cancer," *Am. Assoc. Cancer Res.*, vol. 1, no. October, pp. 1730–1736, 2013.
- [29] N. Bhalla, P. Jolly, N. Formisano, and P. Estrela, "Introduction to biosensors," *Essays Biochem.*, no. June, pp. 1–8, 2016.
- [30] H. H. Nguyen, J. Park, S. Kang, and M. Kim, "Surface plasmon resonance: A versatile technique for biosensor applications," *Sensors*, vol. 15, no. 5, pp. 10481–10510, 2015.
- [31] G.-J. Graulus, "Towards degradable photonic biosensors for the microbiological screening of water samples," Ghent University, 2018.
- [32] B. Wootla, A. Denic, and M. Rodriguez, "Chapter 5 Polyclonal and Monoclonal Antibodies in Clinic," in *Human Monoclonal Antibodies: Methods and*

- Protocols*, vol. 1060, M. Steinitz, Ed. Springer Science+Business Media, 2014, pp. 79–110.
- [33] R. W. Glaser, "Antigen-antibody binding and mass transport by convection and diffusion to a surface: A two-dimensional computer model of binding and dissociation kinetics," *Analytical Biochemistry*, vol. 213, no. 1. pp. 152–161, 1993.
- [34] J. Punt, S. Stranford, P. Jones, and J. A. Owen, *Kuby Immunology*, Eighth. W.H. Freeman & Co Ltd, 2018.
- [35] M. N. Baeshen *et al.*, "Production of Biopharmaceuticals in *E. coli*: Current Scenario and Future Perspectives," *JMB*, vol. 25, no. 7, pp. 953–965, 2015.
- [36] O. Gileadi, *Heterologous Gene Expression in E.coli*, vol. 705. Springer Science+Business Media, 2011.
- [37] P. H. N. Celie, A. H. A. Parret, and A. Perrakis, "Recombinant cloning strategies for protein expression," *Curr. Opin. Struct. Biol.*, vol. 38, pp. 145–154, 2016.
- [38] J. W. Dale, M. Von Schantz, and N. Plant, "How to clone a gene," in *From genes to genomes: Concepts and Applications of DNA Technology*, Third., Surrey: Wiley, 2012, pp. 25–74.
- [39] OpenStax, "Prokaryotic Gene Regulation," *Biology*, 2012. [Online]. Available: [https://cnx.org/contents/GFy\\_h8cu@11.8:drSgdNIj@6/Prokaryotic-Gene-Regulation](https://cnx.org/contents/GFy_h8cu@11.8:drSgdNIj@6/Prokaryotic-Gene-Regulation).
- [40] B. Billen *et al.*, "Cytoplasmic versus periplasmic expression of site-specifically and bioorthogonally functionalized nanobodies using expressed protein ligation," *Protein Expr. Purif.*, vol. 133, pp. 25–34, 2017.
- [41] L. Liang and D. Astruc, "The copper(I)-catalyzed alkyne-azide cycloaddition (CuAAC) 'click' reaction and its applications. An overview," *Coord. Chem. Rev.*, vol. 255, no. 23–24, pp. 2933–2945, 2011.
- [42] J. L. Brunelle and R. Green, *One-dimensional SDS-polyacrylamide gel electrophoresis (1D SDS-PAGE)*, 1st ed., vol. 541. Elsevier Inc., 2014.
- [43] "Protein Expression & Analysis: impact kit, instruction manual," 2019.
- [44] H. M. M. Sadeghi *et al.*, "Optimization of the expression of reteplase in *Escherichia coli*," *Res. Pharm. Sci.*, vol. 6, no. 2, pp. 87–92, 20AD.
- [45] I. Palmer and P. T. Wingfield, "Preparation and Extraction of Insoluble (Inclusion-Body) Proteins from *Escherichia coli*," *Natl. Institutes Heal.*, pp. 1–24, 2012.
- [46] P. Béguin, "How can I detect inclusion bodies in my bacterial cultures," 2016. [Online]. Available: [https://www.researchgate.net/post/How\\_can\\_I\\_detect\\_inclusion\\_bodies\\_in\\_my\\_bacterial\\_cultures](https://www.researchgate.net/post/How_can_I_detect_inclusion_bodies_in_my_bacterial_cultures). [Accessed: 23-May-2019].
- [47] Y. Wang, Z. Wang, Y. Duo, X. Wang, J. Chen, and J. Chen, "Gene cloning, expression, and reducing property enhancement of nitrous oxide reductase from *Alcaligenes denitrificans* strain TB," *Environ. Pollut.*, vol. 239, pp. 43–52, 2018.

- [48] G. Sezonov, D. Joseleau-Petit, and R. D'Ari, "Escherichia coli physiology in Luria-Bertani broth," *J. Bacteriol.*, vol. 189, no. 23, pp. 8746–8749, 2007.
- [49] J. C. Lessard, *Growth media for E. coli*, 1st ed., vol. 533. Elsevier Inc., 2013.
- [50] Bio-World, "NZ Amine A." [Online]. Available: [https://www.bio-world.com/productinfo/3\\_43\\_287\\_688/5997/NZ-Amine-A.html](https://www.bio-world.com/productinfo/3_43_287_688/5997/NZ-Amine-A.html). [Accessed: 23-May-2019].
- [51] Corning, "Troubleshooting : Protein Electrophoresis," 2012.

## Appendices

Appendix A: Results of the first purification experiment.....	50
Appendix B: Results of the second purification experiment .....	52
Appendix C: Results of the third purification experiment .....	53

## Appendix A: Results of the first purification experiment

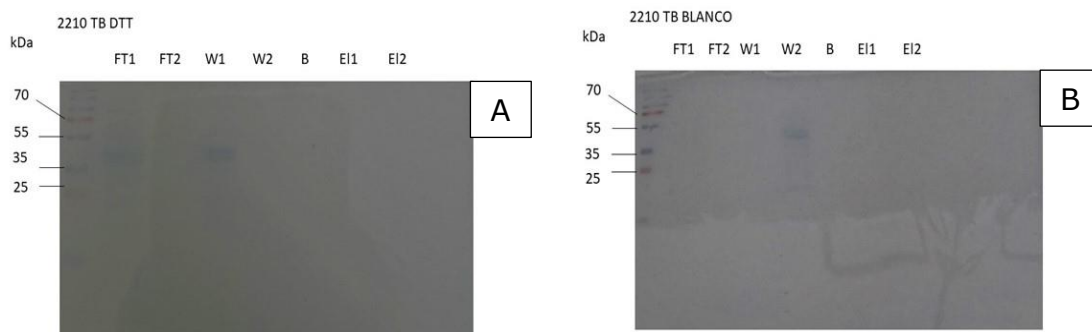


Figure 16: Purification SDS-PAGE results of strain 2210. **A**: results of the column that was treated with cleavage buffer DTT. **B**: results of the column that was treated with column buffer

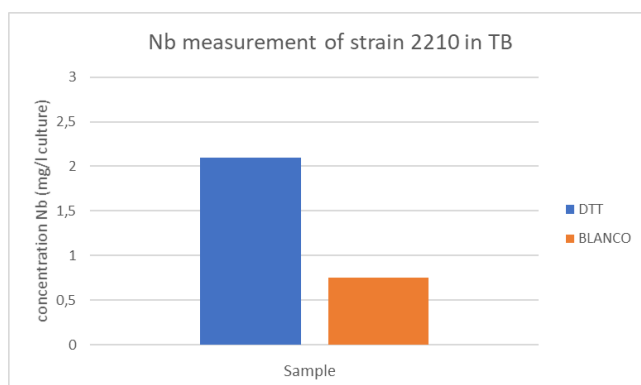


Figure 17: Results of the Nb concentration measurements through Nanodrop of strain 2210

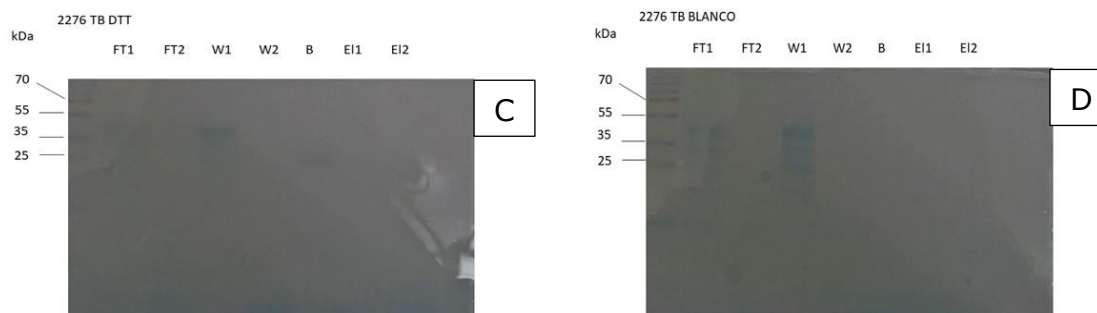


Figure 18: Purification SDS-PAGE results of strain 2276. **C**: results of the column that was treated with cleavage buffer DTT. **D**: results of the column that was treated with column buffer

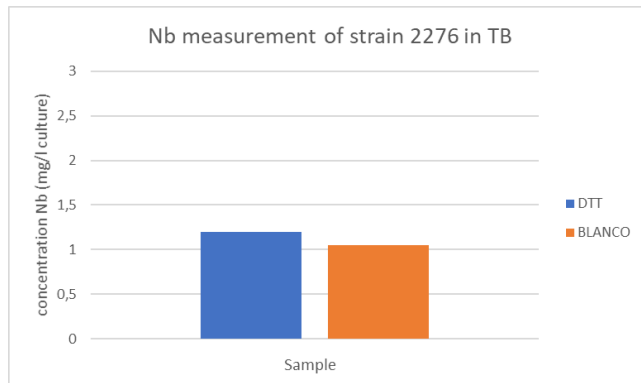


Figure 19: Results of the Nb concentration measurements through Nanodrop of strain 2276

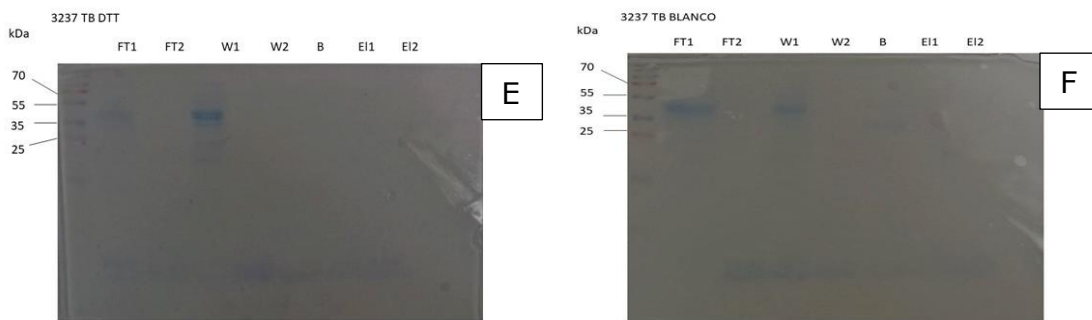


Figure 20: Purification SDS-PAGE results of strain 3237. **E**: results of the column that was treated with cleavage buffer DTT. **F**: results of the column that was treated with column buffer

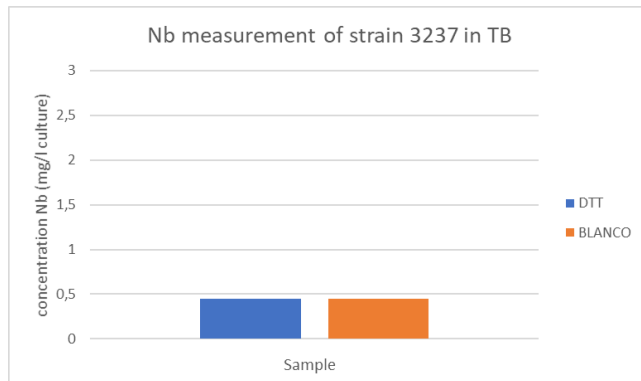


Figure 21: Results of the Nb concentration measurements through Nanodrop of strain 3237

## Appendix B: Results of the second purification experiment

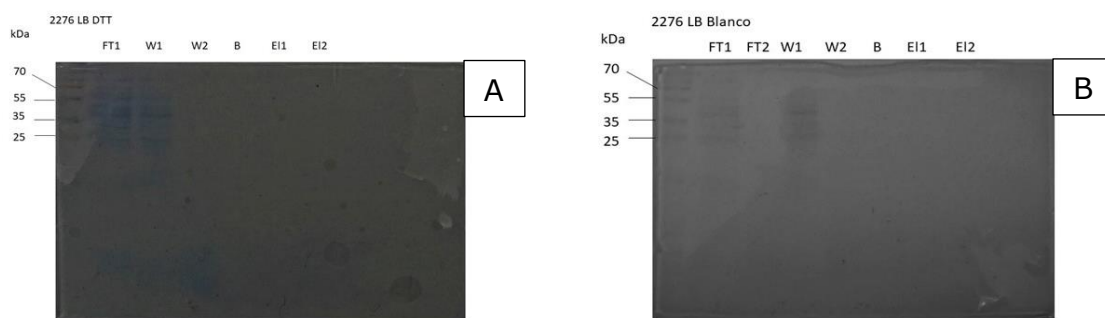


Figure 22: Purification SDS-PAGE results of strain 2276. **A**: results of the column that was treated with cleavage buffer DTT. **B**: results of the column that was treated with column buffer

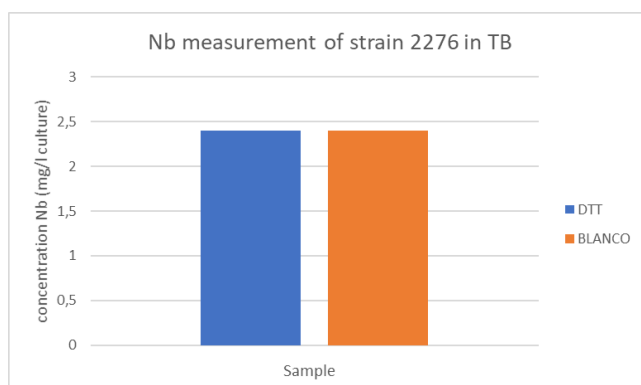


Figure 23: Results of the Nb concentration measurements through Nanodrop of strain 2276

Appendix C: Results of the third purification experiment

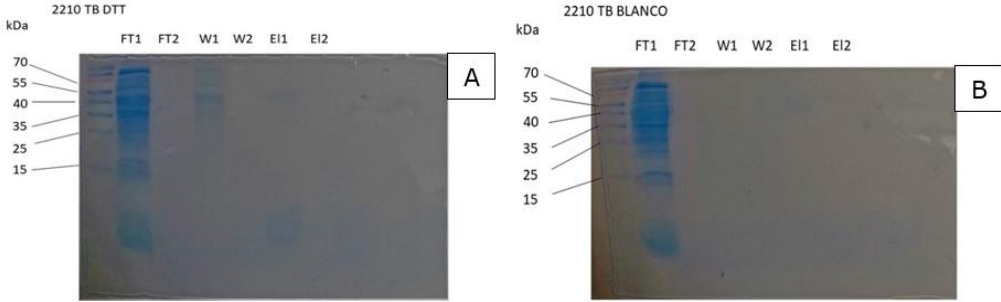


Figure 24: Purification SDS-PAGE results of strain 2210. **A**: results of the column that was treated with cleavage buffer DTT. **B**: results of the column that was treated with column buffer

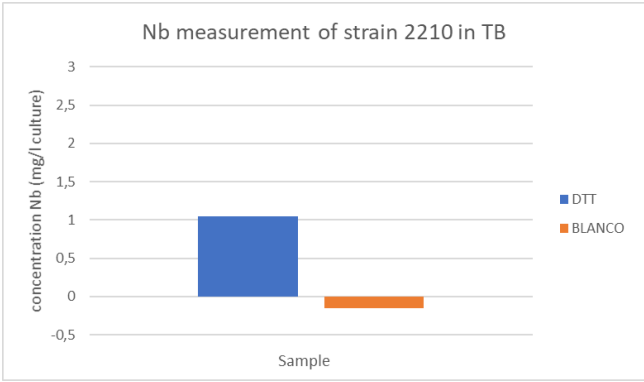


Figure 25: Results of the Nb concentration measurements through Nanodrop of strain 2210

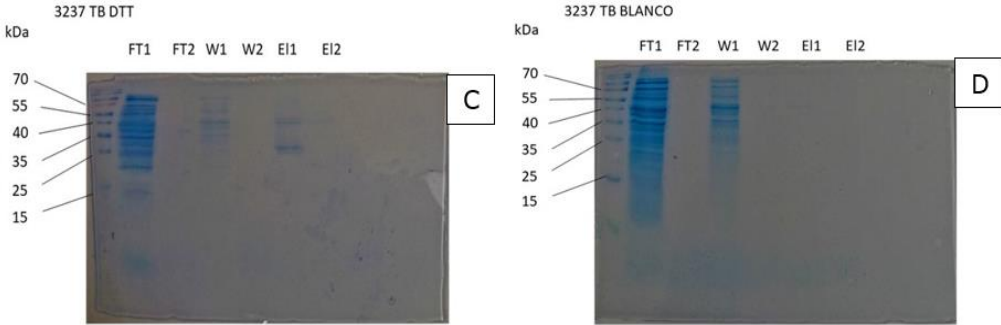


Figure 26: Purification SDS-PAGE results of strain 3237. **C**: results of the column that was treated with cleavage buffer DTT. **D**: results of the column that was treated with column buffer



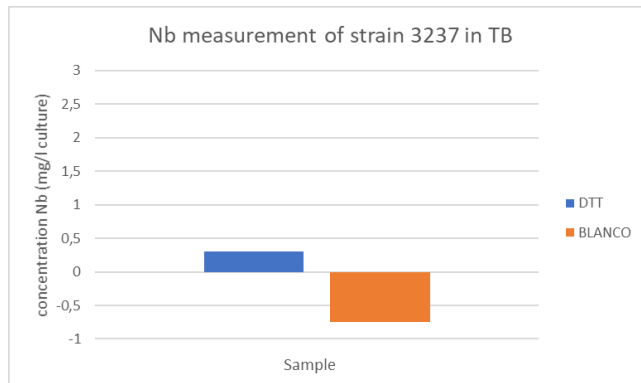


Figure 27: Results of the Nb concentration measurements through Nanodrop of strain 3237

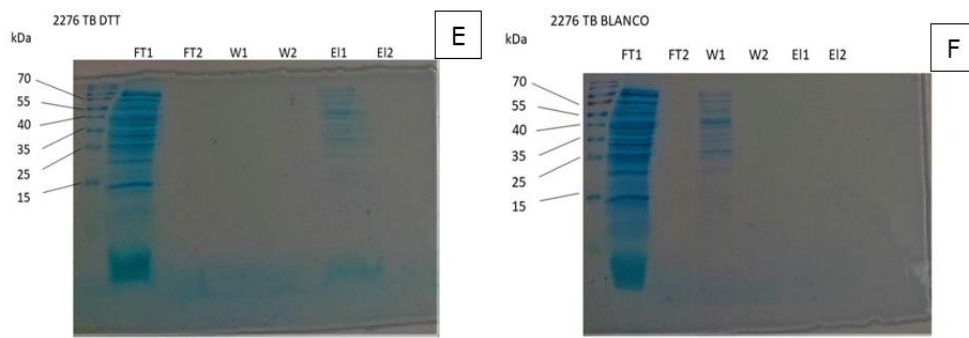


Figure 28: Purification SDS-PAGE results of strain 2276. **E**: results of the column that was treated with cleavage buffer DTT. **F**: results of the column that was treated with column buffer

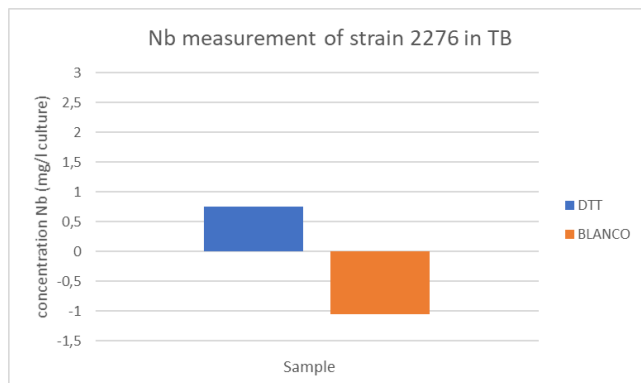


Figure 29: Results of the Nb concentration measurements through Nanodrop of strain 2276